

Block co-polymer self-assembly

by

Areej Alameer

A thesis

presented to the University of Waterloo

in fulfillment of the

thesis requirement for the degree of

Master of Applied Science

in

Electrical and Computer Engineering- Nanotechnology

Waterloo, Ontario, Canada, 2017

© Areej Alameer 2017

AUTHOR'S DECLARATION

I hereby declare that I am the sole author of this thesis. This is a true copy of the thesis, including any required final revisions, as accepted by my examiners. I understand that my thesis may be made electronically available to the public.

Abstract

Contemporary electronic industry heavily relies on its capability to fabricate electronic devices with small feature size. The race to fabricate higher number of electronic devices per area has faced critical miniaturization challenges. In order to meet the increasing demand of industry for fabrication of smaller electronic devices, new methods were being studied and developed to deal with challenges in fabrication of the very small. Nanotechnology and application of nanomaterials is one of the alternative avenues for fabrication of such miniature structures. For many decades, photolithography has been the core of semiconductor industry and device fabrication. However, to meet the industry requirements and deal with miniaturization challenges, variety of photolithography techniques coupled with nanotechnology has been studied and developed. One of such nanotechnology driven techniques that has significantly attracted researchers as well as the semiconductor industry stake holder's attention is bottom-up method based on self-assembly of nanoparticles. Low processing cost, high resolution and large scale processing compatibility are among the prominent advantages of this method.

This thesis mainly focuses on explaining the application of block copolymer (BCP) self-assembly in nanolithography, and their ability to phase separate into ordered and chemically distinct domains of 10s nm size. Moreover, this thesis presents an effective way to obtain a perpendicular self-assembled PS-b-PMMA with very high aspect ratio which is preferred for pattern transfer. To deliver this unique orientation, 3-MPTS is used to neutralize the surface. This method depends on vapor deposition of 3-MPTS at room temperature for two hours or less prior to deposition of PS-b-PMMA.

Acknowledgements

First and foremost, I would like to thank my Supervisor, Professor Bo Cui, for all his support and guidance. Without his dedicated efforts throughout my study and research, this work would not have been achieved. His guidance, patience, enthusiasm and dedication to research helped me to face and overcome all the challenges that I encountered during my M.Sc Studies.

I would like also to thank all my research group members for their help and support throughout my studies. I would like also to express my heartfelt gratitude to Ritchard Barber the manager of G2N lab, towards aiding me to overcome the laboratory concerns and limiting the technical issues.

I cannot express my deepest thanks and appreciation to my parents, Hassan Alameer and Mariam alameer for their support and encouragement throughout my study. Literally without their tireless efforts, I would never be where I am now. The same appreciation extends to my sisters and brothers for their tremendous emotional and financial support. I wholeheartedly thank all of them for being always engaged.

Special acknowledgment goes to my most ambitious friend Farah Alshehri, for her unwavering love and constant attention and support. Her encouraging sayings and loyal prayers helped me to overcome the difficult feeling of homesickness and kept my motivation levels high whenever I was overwhelmed.

Finally, deepest thank and prayer to the Saudi king, his majesty Abdel-Allah, may Allah have mercy on him, for offering me the greatest opportunity ever of a fully granted scholarship, which has enabled me to undertake my higher education.

Also, the continuous assistance from the Saudi Arabian Cultural Bureau in Canada is also gratefully acknowledged, with special appreciation for both supervisors, Dr. Mohamad Najem and Dr. Yousef Abu-Nada, for their great supervision and help for all Saudi students including myself.

Dedication

This thesis is dedicated to my mother Mariam Alameer and my father Hassan Alameer for their love, endless support and encouragement.

Table of Contents

AUTHOR'S DECLARATION	ii
Abstract	iii
Acknowledgements	iv
Dedication	vi
Table of Contents	vii
List of Figures	ix
List of Tables	xi
Introduction.....	1
Thesis overview	3
Chapter 1. Block Copolymers	4
1.1 Block Copolymer Self-Assembly.....	5
1.2 Key Components Of Self Assembly	6
1.3 Block Copolymer Thin-Films	7
1.3.1 Thin Film Deposition.....	7
1.4 Block Copolymer Thin Films Wettability.....	8
1.5 BCP Morphologies In Thin Film	9
1.5.1 Lamellae Morphology In Thin Films.....	9
1.5.2 Cylindrical Morphology In Thin Tilms	11
1.5.3 Spherical Morphology In Thin Films	11
1.6 Controlling The Out-of-Plane Orientation	11
1.7 Neutralization By The Use Of Monolayers.....	12
1.8 Corrugated Surfaces	13
1.9 Addition Of Additives In The BCP	14
1.10 Applying External Forces.....	14
1.11 Solvent Casting Of The Block Copolymers	16
1.12 Thickness Gradient	16
1.13 Mechanical Flow Fields.....	17
1.14 Temperature Gradient.....	18
1.15 PS-b-PMMA Thin Film.....	20
1.16 Pattern Transfer Method.....	21
1.16.1 Dry Etching.....	22
1.16.2 Wet Etching	25

1.17	Conclusion	27
Chapter 2.	Experimental Work and Results	28
2.1	Introduction	28
2.2	Preparation Of PS-b-PMMA Film	28
2.3	Deposition Of Aluminum On Top Of The Silicon Wafer.....	28
2.4	Coating PS-b-PMMA BCP Thin Film With A Surface Neutralizing Underlayer	29
2.5	Varying Annealing Time To Form Self-assembly Of Block Copolymer	33
2.6	The Effect Of The Soaking Time	37
Chapter 3.	Discussion and Findings	52
3.1	Coating PS-b-PMMA BCP Thin Film	52
3.2	Coating PS-b-PMMA BCP Thin Film With A Surface Neutralizing Underlayer	52
3.3	Varying The Annealing Time To Form Self-assembly of Block Copolymer.....	54
3.4	Varying Soaking And RIE Etching Time	54
3.5	Conclusion.....	55
Bibliography	56

List of Figures

Figure 1: Different classes of copolymers. 1) Homo-polymer. 2) Alternating copolymer. 3) Random copolymer. 4) Block copolymer. 5) Graft polymer.	4
Figure 2: Formation of different micro-phase domains in block copolymer mix.	5
Figure 3: Preferential wetting of the substrate. 1) Lamellae structure parallel to the substrate. 2) Lamellae structure perpendicular to the substrate [1].	8
Figure 4: Schematics of symmetric and asymmetric wetting of the substrate for the lamellar phase.....	10
Figure 5: Induced upright orientation for a corrugated surface	13
Figure 6: Schematic of high-density nanowire fabrication in a polymer matrix. (a) An asymmetric diblock copolymer annealed above T_g under an applied electric field, forming a hexagonal array of cylinders oriented normal to the film surface. (b) After removal of the minor component, a nanoporous film is formed. (c) By electrodeposition, nanowires can be grown in the porous.....	15
Figure 7: Thickness gradient of poly(styrene- <i>b</i> -butadiene- <i>b</i> -styrene) triblock copolymer. Parts (a) and (b) are phase SPM images of the triblock copolymer which reconstructs as a function of film thickness. Part (c) is a schematic height profile of the phase images shown above, while part (d) is a simulation of the same block copolymer [1-5].	17
Figure 8: Chemical structure of PMMA- <i>b</i> -PS.	20
Figure 9: (a) Isotropic etching of silicon(b) Partially anisotropic and (c) Completely anisotropic.....	21
Figure 10: the plasma hits the silicon wafer with high energy to knock-off the Si atoms on the surface. (a) The plasma atoms hitting the surface. (b) The silicon atoms being evaporated off from the surface. [18].....	22
Figure 11: Process of a reactive ion interacting with the silicon surface. (a) The interaction between the reactive ion and the silicon atom. (b) A bond between the reactive ion and the silicon atom then chemically remove the silicon atoms from the surface. [18]	23
Figure 12: Pattern transfer using the PS- <i>b</i> -PMMA block copolymer as an etching mask.....	24
Figure 13: Schematics of an etch profile in (a) an anisotropic and (b) an isotropic etch of a (100) oriented silicon surface. (c-d) KOH based wet etching of (110)- oriented Si surfaces with micro and nanoscale two-dimensional walls. [18]	26
Figure 14: A schematic of the chemical structure of 3-(<i>p</i> -methoxy phenyl) propyl trichloro silane (3-MPTS).....	29
Figure 15: Schematic of PS- <i>b</i> -PMMA BCP.	30
Figure 16: AFM image of self-assembly on PS- <i>b</i> -PMMA after 3MPTS treatment	31
Figure 17: SEM image of the self-assembled of BCP with low coverage of 3MPTS	32
Figure 18: optical microscopy image of thin film after annealing.	32
Figure 19: SEM image of the self-assembled of BCP with high coverage of 3MPTS.....	33
Figure 20: AFM image of annealed BCP at 190 °C for 20 min.....	34
Figure 21: SEM image of annealed BCP 19.1 at 190 °C for 20 min.	34
Figure 22: SEM image of annealed BCP 65.6 kg/mol at 190 °C for 20 min.	35
Figure 23: SEM image of annealed BCP 33kg/mol at 190 °C for 1 hour.....	35
Figure 24: SEM image of annealed BCP 65kg/mol at 190 °C for 1 hour.....	36
Figure 25: SEM image of annealed BCP 33kg/mol at 190 °C for 3 hours.	36
Figure 26: SEM image of annealed BCP 65 at 190 °C for 3 hours.	37
Figure 27: A) schematic of self-assembled lamella on silicon surface. B) After treat with HAC. C) After treated with mixed acid and RIE.....	38
Figure 28: Ps- <i>b</i> -PMMA 19.1 kg/mol after 5 seconds soaking.	39
Figure 29: Ps- <i>b</i> -PMMA 19.1 kg/mol after 10 seconds soaking.	40
Figure 30: Ps- <i>b</i> -PMMA 19.1 kg/mol after 12 seconds soaking.	40
Figure 31: Ps- <i>b</i> -PMMA 19.1 kg/mol after 15 seconds soaking.	41
Figure 32: Ps- <i>b</i> -PMMA 19.1 kg/mol after 25 seconds soaking.	41
Figure 33: Ps- <i>b</i> -PMMA 19.1 kg/mol after 35 seconds soaking.	42
Figure 34: Ps- <i>b</i> -PMMA 19.1 kg/mol after 40 seconds soaking.	42
Figure 35: Ps- <i>b</i> -PMMA 19.1 kg/mol after 60 seconds soaking.	43
Figure 36: Ps- <i>b</i> -PMMA 19.1 kg/mol after 5 minutes soaking.	43
Figure 37: Ps- <i>b</i> -PMMA 19.1 kg/mol after 10 minutes soaking.	44

Figure 38: <i>Ps-b-PMMA 19.1 kg/mol after 15 minutes soaking.</i>	44
Figure 39: <i>Ps-b-PMMA 19.1 kg/mol after 20 minutes soaking.</i>	45
Figure 40: <i>SEM image of etched is structure after RIE (treated time 5 seconds)</i>	46
Figure 41: <i>SEM image of etched is structure after RIE (treated time 5 seconds)</i>	46
Figure 42: <i>SEM image of etched is structure after RIE (treated time 15 seconds)</i>	47
Figure 43: <i>SEM image of etched is structure after RIE (treated time 20 seconds)</i>	47
Figure 44: <i>SEM image of etched is structure after RIE (treated time 25 seconds)</i>	48
Figure 45: <i>SEM image of etched is structure after RIE (treated time 35 seconds)</i>	48
Figure 46: <i>SEM image of etched is structure after RIE (treated time 40 seconds)</i>	49
Figure 47: <i>SEM image of etched is structure after RIE (treated time 60 seconds)</i>	49
Figure 48: <i>SEM image of etched is structure after RIE (treated time 10 minutes).</i>	50
Figure 49: <i>SEM image of etched is structure after RIE (treated time 20 minutes).</i>	50
Figure 50: <i>SEM image of etched is structure after RIE (treated time 30 minutes).</i>	51
Figure 51: <i>a) Horizontal self-assembled lamella on a non-neutralized silicon surface. b) Vertical self-assembled lamella on a neutralized silicon surface (the green area represents 3-MPTS monolayer)</i>	53

List of Tables

<i>Table 1: Summary of common methods to orient the micro domains later and/or perpendicular to the substrate surface [1-6].</i>	19
<i>Table 2: Flory–Huggins parameter for different BCPs [1-15].</i>	21

Introduction

In order to meet Moore's law, we need to develop alternative fabrication technologies [1-2]. In semiconductor industry, current research and developments are focused on developing devices with minimum size using different upgraded lithographic techniques [2-4]. The state-of-the-art immersion photolithography technology is now limited to ~10 nm feature size [1]. Photolithography, even with state-of-the-art 193 nm immersion technology with multiple-patterning ability, is unable to scale well below 10 nm. [2-1]. The alternative approaches to photolithography is bottom up approach based on self-assembly [2]. In this regards, block copolymer (BCP) self-assembly has attracted serious attentions in last two decades to achieve better results for a variety of applications such as nanolithography, nanotemplating, nonporous membranes and ultra-high density storage media [1]. In this approach, the chemical properties of the materials are modified or sometimes one of the components is selectively removed to form the desired structures by self-assembly of the molecules [1]. Currently, feature sizes down to 3nm can be achieved from the self-assembly of BCPs, and potentially even smaller feature sizes are achievable [2].

International Business Machines Corporation (IBM) [4-10], and Hitachi Global Storage Technologies (HGST) [4-11] have announced the first manufacturing application of BCP self-assembly in a conventional chip fabrication line. However, there are many challenges associated with the application of BCPs for nanofabrication [1].

Challenges associated with application of BCPs in nanofabrication are:

1. Generally, BCPs are self-assembled in an isotropic manner in the absence of surface forces

and external fields [1].

2. There are very few self-assembled BCPs which can reach domains that are smaller than 10nm and still maintain their properties.
3. BCPs are excellent for high throughput and large scale device fabrication for industrial application, but the annealing process of BCPs takes days to hours and limit this technology for commercial use [1]. Moreover, obtaining directed self-assembled structure can be very expensive because of the high cost of instruments and processing setups such as e-beam lithography, which requires a large amount of capital and is more time consuming when it comes to fabrication of large area structure [1].

Many researchers have developed different technologies to direct the self-assembly of BCP film. Among technologies, graphoepitaxy, chemical pre patterning, solvent annealing, mechanical flow fields, electric or magnetic fields, thermal gradients, and salt doping or homopolymer blending and surface wettability control have shown promising results [1].

Thesis overview

In this thesis, a general introduction to BCP lithography and pattern-transfer techniques is provided in chapter 1. This is followed by presenting details of our experimental work. In chapter 2, a novel surface treating method to neutralize the surface energy and to control the BCP's orientation and morphology is introduced. Self-assembled monolayer (SAM) of 3-MPTS was evaporated on the substrate to wet both blocks of the BCP thin film. Then PS-b-PMMA morphology under different time and constant temperature was studied. In chapter 3, finally we conclude by discussing the challenges and our findings in this research.

Chapter 1. Block Copolymers

Copolymer is formed from two different monomers A and B. By rearrangement of these monomers, the copolymers are classified in five different classes: homo-polymer, alternating copolymer, random copolymer, block copolymer and graft polymer. The structure of these copolymer categories is shown in fig 1. A single monomer combines to form polymer chain is called homopolymer. Two different monomers A and B arranged in alternative way along polymer chain is called alternative copolymer as shown in figure 1(2). In random copolymer, two monomers may arrange themselves in any order to create copolymer chain (see figure 1(3)). Block copolymers are linear polymer with two sequences of each monomer A and B (BCP) (see figure1(4)). In other word, (BCP) is two homopolymer subunit linked together by covalent bond. In graft copolymers, the main chain includes only one monomer and the other monomer form side chains grafted to the main chain.



Figure 1: Different classes of copolymers. 1) Homo-polymer. 2) Alternating copolymer. 3) Random copolymer. 4) Block copolymer. 5) Graft polymer.

1.1 Block Copolymer Self-Assembly

Block copolymer is consist of two homopolymers linked together by covalent bond. Due to non-favorable segmental interactions, copolymers undergo what is termed “micro-phase separation” and create nanoscale domain [2]. When micro-phase separation occurs, the nanoscale domains are not randomly located. Accordingly, the nanoscale structures can form variety of periodic structure at certain volume fraction and polymer chain length as shown in fig 2[1-3].

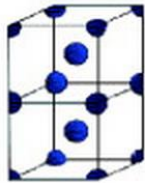
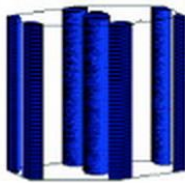
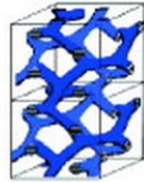
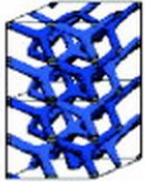

Nature of patterns	Spheres (SPH) (3D)	Cylinders (CYL) (2D)	Double gyroid (DG) (3D)	Double diamond (DD) (3D)	Lamellae (LAM) (1D)
Space group	$Im\bar{3}m$	$p6mm$	$Ia\bar{3}d$	$Pn\bar{3}m$	pm
Blue domains: A block					
Volume fraction of A block	0-21%	21-33%	33-37%	33-37%	37-50%

Figure 2: Formation of different micro-phase domains in block copolymer mix.

As it is shown in the figure, the shape of nanoscale domain depends on the volume fraction (f). Upon adjusting the volume fraction of polymer blocks, one of the following shapes can be obtained: spherical, cylindrical, gyroid, diamond and lamellar. Thin film containing these self-assembled patterns are considered as nanolithographic masks as well as templates for the further synthesis of inorganic or organic structures [5]. By knowing the molecular weight of block copolymer chain and the shape of domains, one can detect the size of micro domains [1-2]. Since

the polymer chains are covalently bonded together, the size scale of the domains must be commensurate with the size of the polymer chain, typically, on the tens of nanometers length scale or less [2].

1.2 Key Components Of Self Assembly

The Flory- Huggins equation is the most proper way to describe self-assembly of Block copolymers:

$$\frac{\Delta G_{\text{mix}}}{k_b T} = \frac{1}{N_A} \ln(f_A) + \frac{1}{N_B} \ln(f_B) + f_A f_B \chi \quad \{1\}$$

Decades of research have provided a foundation for understanding block copolymer self-assembly. In equation {1}, (χ) represents the A-B Flory-Huggins interaction parameter, (N) represents degree of polymerization and block volume fractions is represented by (f) [6].

The equation shows that the Gibbs free energy of the system which indicates whether BCPs phase separate or not, is proportional to the degree of polymerization (N), volume fraction of the polymers (f), and the Flory-Huggins interaction parameter (χ).

The block copolymers phase separation into periodic micro-domains is determined by the strength of the repulsive interaction as characterized by the product χN . Micro-phase separation can occur when this value exceeds the critical value of $\chi N > 10.5$ for the order-disorder transition [6]. If $\chi N < 10.5$, then the blocks of the BCP will mix, forming a homogeneous or phase-mixed morphology. This means that to decrease the size of the micro-domains and maintain a micro phase-separated morphology, N must decrease and χ must increase to compensate [5].

1.3 Block Copolymer Thin-Films

After discussing the properties of BCPs, we need to highlight the effective utilization of BCP in fabrication of nanostructure by thin film deposition of BCP on a substrate for different applications such as patterned magnetic, recording media, and nanowire arrays [1].

1.3.1 Thin Film Deposition

There are various methods for coating BCP film on a substrate. The first common method for BCP thin films preparation is the drop casting method. In this method, BCP is dissolved in a proper solvent and few drops are placed on the substrate to dry. This would leave drying spots and non-uniform coverage [1].

The second method is the dip coating method, for which the substrate is dipped into BCP solution and taken out. After evaporation of the solvent, the substrate will be covered with the thin film. In this method, there is no control on the film thickness. Also this method often leads to more non-uniform coverage [1].

The most common method is the spin coating. This process requires a polymeric solution (~1% by weight) and a spinning substrate. Few drops are placed on the substrate then the spinning speed and time are adjusted to obtain specific thickness and homogenous coverage of the film. Film thickness is controlled by the spinning speed, concentration of the solution and molecular weight of the BCP.

Typically, after BCP coating, films are annealed so that the solvent is driven away from the film. Annealing also allows the polymer segments to move and the phase to separate faster [1-4].

1.4 Block Copolymer Thin Films Wettability

It is critical to form structure that is vertical to the substrate in different application of nanofabrication. As shown in fig 3, A-B is spin coated on a substrate with a final goal to achieve lamellae structure. However, there are two ways for lamellae structure to orient itself, either vertical or horizontal to the substrate surface [1].

In order to achieve horizontal lamellae orientation, substrate should have a preferential wetting affinity for one of polymeric blocks either A or B. In this case, the preferred block will be attached to the substrate first, and then another block will be followed the same direction as the underlying block [1]. Figure 3-1 shows the preferential wetting of block B and its horizontal orientation. It is important to note that if block A was preferred by the substrate it will be attached to the substrate first and would reverse the ordering of the polymers in the horizontal orientation [1].

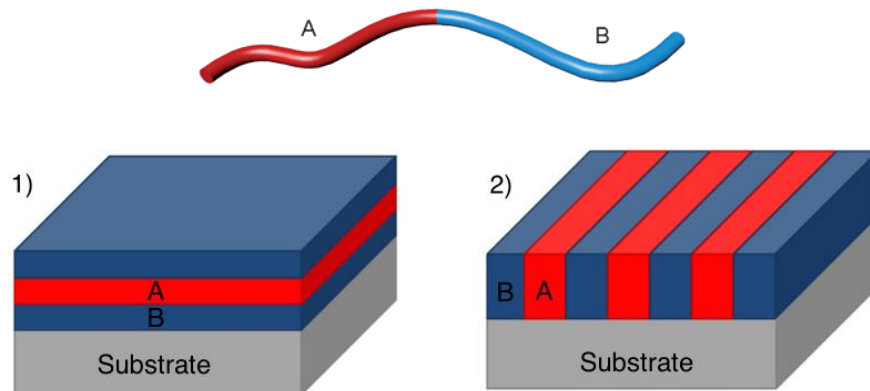


Figure 3: Top, schematic of typical block copolymer. Preferential wetting of the substrate. 1) Lamellae structure parallel to the substrate. 2) Lamellae structure perpendicular to the substrate [1].

Both blocks should have a similar affinity for wetting the substrate to achieve the vertical lamellae. More clearly, each block copolymer must have the same opportunity to wet the substrate, only under this condition a vertical ordination is possible (see figure 3-2).

The factors that control the wetting characteristic of a substrate are: a) composition, b) hydrophobicity and hydrophilicity, c) surface charges [1]. These factors can affect the surface energy of the substrate and the wetting affinity of the BCPs. A novel surface energy modification method is utilized to neutralize the surface energy of the silicon substrate, and to promote the vertical alignment of the BCP micro-domains [1].

1.5 BCP Morphologies In Thin Film

In the thin films, the formation of BCP depends on two factors. First, the interaction of the films with interfaces (Air / Substrates). Second, the compatibility of periodicity of the BCP blocks with the film thickness [1-6].

In contrast to the bulk BCPs, in thin films that are thick enough to accommodate multiple domain layers, the micro-domains do not follow the same pattern near the interfaces of the film. The interlayer spacing can be affected especially in the layers closest to the interfaces bounding the thin film (Air/Substrate). In this section, we present the effect of these two factors on the formation of various BCP morphologies in thin films [1].

1.5.1 Lamellae Morphology In Thin Films

In lamellae morphology, each interface (Air/ substrate) has affinity to wet one of block

copolymer, thus the block that has higher affinity will align itself parallel to the respective interface [1]. For the symmetric wetting condition, the same block wets both surfaces (figure 4.a), thus film thicknesses (d) must quantize to integer multiples (n) of the lamellae spacing (L_0), $d = nL_0$ [10]. However, for the asymmetric wetting where the two surfaces are not wetted by the same block (figure 4.b), film thicknesses must be quantized to $d = (n+1/2)L_0$ [1]. If the film thickness does not follow these conditions, then islands and holes (or “terraces”) will be formed. This is due to the fact that energetic penalty for creating more film surface area is less than the penalty caused by altering the domain periodicity (chain stretching or compression) or by putting an energetically disfavored block in contact with one or both surfaces. If $d < L_0$, perpendicular morphologies are possible [1-7].

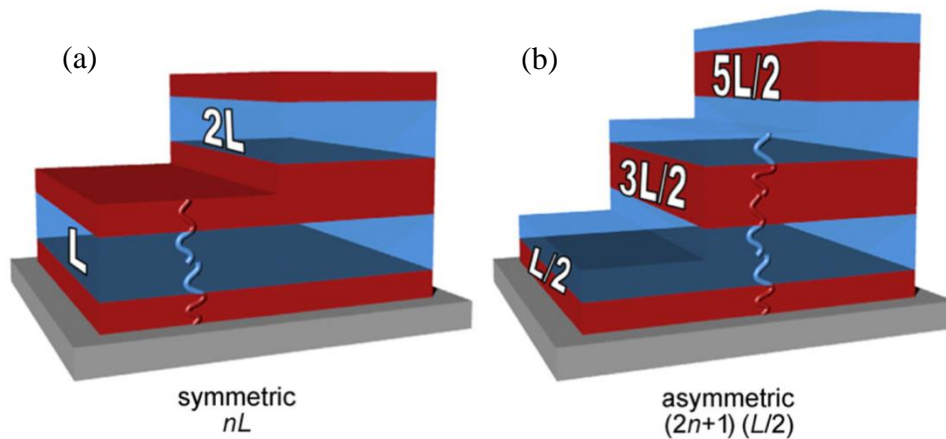


Figure 4: Schematics of symmetric and asymmetric wetting of the substrate for the lamellar phase.

1.5.2 Cylindrical Morphology In Thin Films

Like lamellae phase, the preferential wetting of the substrate by one of the blocks will orient the cylinders parallel to the surface. If the surface has higher affinity for the minority block, a brush like structures (perpendicular cylinders) will form [1-7]. Similarly, for the cylindrical phase, discrete film thicknesses are allowed. If the thickness does not follow the discrete thicknesses, then interesting morphologies such as perpendicularly oriented cylinders and perforated lamellar structures form [1-7]. At certain thicknesses the cylindrical morphology will transfer to a close-packed spherical morphology because of the high-energy cost of distorting the cylinders away from their preferred spacing.

1.5.3 Spherical Morphology In Thin Films

If the minority block wets the surface, the micro domains will attach themselves parallel to the surface. In bulk, the spheres are packed into a bcc lattice, however in thin films, a monolayer of spheres is packed into a close-packed configuration, which may be viewed as a distorted $\langle 110 \rangle$ plane of the bcc structure, as there are no longer any neighboring layers to break the in-plane symmetry [1-7].

1.6 Controlling The Out-of-Plane Orientation

In many nanofabrication applications, the orientation of micro domains in thin films are very important. In the case of dry etching, that is widely used to pattern transfer, to achieve a certain

depth either the thickness of the etching mask or the selectivity of the mask compared to substrates is very crucial. Micro domains with upright orientation allow a better control for etching because they have a high aspect ratio and are better for pattern transfer. However, forming micro-domains with perpendicular orientation is challenging due to the naturally block components of BCPs which have different affinity for the bounding interfaces (air/substrate).

This preferential wetting mechanism, as discussed in the previous section, leads to parallel orientation of the domains rather than the perpendicular orientation. In order to achieve this unique orientation, blocks must not show preferential affinity for either surface. In this section, we present the most effective ways to obtain the perpendicular orientation [1].

1.7 Neutralization By The Use Of Monolayers

Many scientists have reported the neutralization of the surface by using different monolayers of material as a primer for the BCP film. A typical method is to graft random block copolymer PS-*r*-PMMA to the surface of the substrate. At this step, we should confirm that the surface energy is naturalized, and the substrate has an equal affinity for both block, promoting the perpendicular orientation of the micro-domains.

Mansky et al. [10] determined the greatest PS content (~60%) in a PS-*r*-PMMA copolymer to neutralize the surface for a lamellae-forming PS-*b*-PMMA [1]. Ham et al. [11] later showed that there were slight difference between the range of PS content in the random copolymer yielding perpendicular cylinders for PS-*b*-PMMA and the range yielding perpendicular lamellae. Peters et al. [12] used self-assembled monolayers of octadecyltrichlorosilane (OTS) that were chemically changed by X rays in the presence of air to produce aldehyde and hydroxyl groups which, at the

proper level, can yield a neutral surface for PS-*b*-PMMA. Kim et al. [13] used self-assembled monolayer (SAM) of silane on silicon substrate to decrease the surface energy and successfully induced the upright orientation of the BCP lamellae and cylindrical morphologies. In the present study, we use similar technique to Kim's method as will be discussed later in more details.

1.8 Corrugated Surfaces

On a rough surface, we can observe the upright orientation. This because the penalty is incurred for elastic deformation to conform to a rough substrate. Sivaniah et al. [14] noticed perpendicular orientations in lamellae-forming PS-*b*-PMMA on a rough substrate [1]. Moreover, chemically patterned surfaces have been generated that have periodic affinities to each block, which causes a lamellae-forming block copolymer to orient perpendicularly to the surface [1]. Figure 5.a indicates the AFM image of diblock copolymer with upright morphology on corrugated substrate. Figure 5.b and 5.c are clarification of the underlying mechanism for the lateral orientation of the micro-domains on corrugated substrate [1].

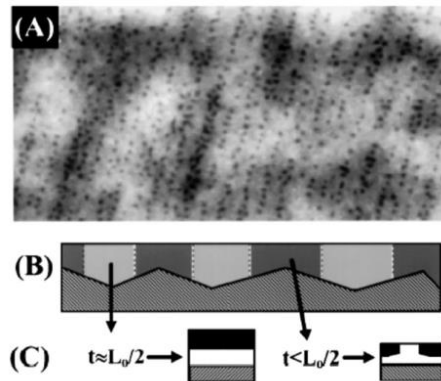


Figure 5: Induced upright orientation for a corrugated surface

1.9 Addition Of Additives In The BCP

The above mentioned reorientation is due to segregation of the additive particles at the interface and mediate the block copolymer/substrate interactions. Lin et al. [1] added cadmium selenide nanoparticles to a cylinder-forming PS-*b*-P2VP block copolymer, which caused reorientation of the micro domains perpendicular to the substrate. A cylinder-forming blend of PS-*b*-PMMA with poly (ethylene oxide)-coated gold nanoparticles (Au-PEO) can be induced to orient perpendicularly to the substrate by annealing in humid air. Jeong et al. [1] indicated that addition of dry-brush PMMA homopolymer to a cylinder-forming PS-*b*-PMMA block copolymer will stabilize the perpendicular orientation of the micro domains in thicker films (hundreds of nanometers). Wang et al. [1] induced a perpendicular orientation of a lamellae-forming block copolymer by adding lithium chloride to PS-*b*-PMMA.

1.10 Applying External Forces

In order to reorient the micro-domains into perpendicular orientation, one may apply electric field to the BCP thin film. Thurn-Albrecht et al. [15] have illustrated the use of electric fields in orienting cylinder-forming PS-*b*-PMMA block copolymers perpendicular to the substrate, with sufficient contrast in dielectric permittivity that exists between these two blocks [1]. In their experiment, electric field was applied to BCP film which was bounded in between two aluminum electrodes with “Kapton spacer” to avoid shorting. Figure 6 shows a schematic of their setup. They have managed to measure the minimum voltage required to obtain upright micro-domains in films with up to 30um [1]. Xu et al. [16] were able to align lamellae-forming PS-*b*-PMMA with an electric field, but it was not for all thicknesses (thin films stubbornly remained parallel, whereas

very thick films, thickness $>10L_0$, had parallel orientations near their surfaces [1].

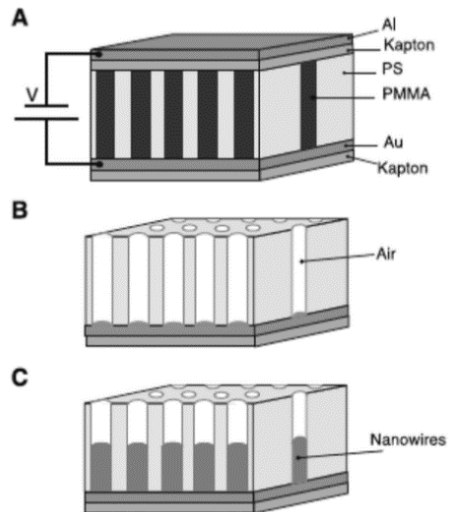


Figure 6: Schematic of high-density nanowire fabrication in a polymer matrix. (a) An asymmetric diblock copolymer annealed above T_g under an applied electric field, forming a hexagonal array of cylinders oriented normal to the film surface. (b) After removal of the minor component, a nanoporous film is formed. (c) By electrodeposition, nanowires can be grown in the porous template [1-12-13].

In thin films, the electric field is useful for fabricating micro-domains perpendicularly oriented to the substrate with high aspect ratio [1].

1.11 Solvent Casting Of The Block Copolymers

Solvent casting of the block copolymer has been indicated to orient micro-domains perpendicular to the substrate due to extremely directional solvent evaporation [1-7]. One of the fundamental factors that determines the orientation of the domains is solvent evaporation rate [1-7]. Another key of this method is that general solvents enhance the mobility of the blocks and speed up the grain growth [1-7]. Many reports for orienting micro-domain have used this method, and a careful temperature control, vapor pressure, and vapor extraction speed must be applied. Moreover, due to the uniaxial degeneracy of perpendicular lamellae and vertically oriented cylinders, this approach cannot result in a good lateral order [1].

1.12 Thickness Gradient

As discussed previously, for the symmetric wetting condition, lamellae structures have a natural repeat spacing of the domain structure of nL_0 , and for the asymmetric wetting condition $(n+1/2)L_0$ [1]. We have observed that if the film thickness is not in proportion to this spacing, a combinations of islands and holes may form. When the film is spun on the substrate, and if the film thickness is matched with the natural thickness of the BCP polymer, a smooth surface is observed for the case of parallel orientation of the BCP film [1]. However if the film thickness does not follow the nL_0 criteria for the symmetric wetting and $(n+1/2)L_0$ for asymmetric wetting, then lamellae phase with perpendicular orientation is obtained [1].

In sphere and cylinder forming block copolymers, when the film thickness is not close matching, islands and holes form. A natural thickness has been given by $h = a*n + b$, where a is

the layer-to-layer distance for the sphere (or cylinder) and b is the thickness of the brush adsorbed on the surfaces (whether such a brush forms) [1].

Figure 7 shows the thickness gradient of the BCPs. In this figure, surface reconstructions of a cylindrical block copolymer including reorientation of nano-domains, wetting layers, and perforated lamellae is clearly observable due to the interplay between surface fields and confinement effects [1-5].

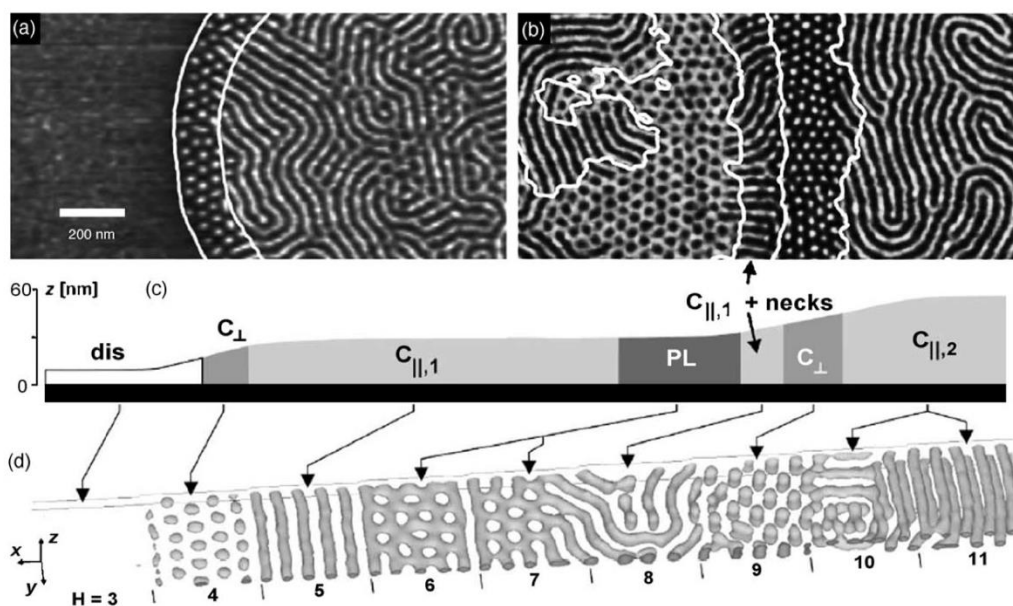


Figure 7: Thickness gradient of poly (styrene-b-butadiene-b-styrene) triblock copolymer. Parts (a) and (b) are phase SPM images of the triblock copolymer which reconstructs as a function of film thickness. Part (c) is a schematic height profile of the phase images shown above, while part (d) is a simulation of the same block copolymer [1-5].

1.13 Mechanical Flow Fields

To aligning the BCP domains, one may use the shear forces to orient the micro-domains.

Albalak et al. [17] have used roll-casting, at which point a block copolymer solution can evaporate whereas an extensional flow is induced between two co-rotating rolls to orient cylinders and lamellae parallel to the extension direction. In this method, films with high thickness of 30um or higher were generated. However, other methods were developed to obtain films with lower thicknesses. Kimura et al. [18] have used the flow of a droplet pinned to a tilted surface in conjunction with solvent evaporation to orient a cylinder forming PS-*b*-PB thin film. The pinning of the drop causes directional flow within the droplet normal to the pinned edge, which induces ordering as the solvent evaporates. Another version of this method is to use sphere forming BCP to create cylindrical micro-domains. In this method sphere forming BCP, which is close to the sphere/cylinder phase boundary is put under the shear force to transform the spheres into cylinders along the direction of the applied force.

1.14 Temperature Gradient

Berry et al. [20] reported a method in which a temperature just below the order disorder temperature and above the glass transition temperature of PS-*b*-PMMA was applied to the BCP film in the direction of the front motion on a rolling substrate. Temperature gradient was created by passing the sample (at a controllable rate) through a hot block between two cold blocks, which produces a bell-shaped temperature profile for each spot in the film as a function of time. The result of this method is to produce a more rapid motion of the defects and increased reorientation of the micro-domains as the velocity of the sample decreased. They refer the ordering to the creation of an in-plane spatiotemporal mobility gradient that biases the grains as they form [18-1].

Table 1 summarizes the most common methods to orient the micro-domains in an upright position for both bulk and thin film forms. Generally, these methods are bottom up approach and

fall under the self-assembly methodology. To produce better and more controllable orientations, other methods can be used such as: epitaxy, directional crystallization of a solvent–polymer solution, and graphoepitaxy. However, these methods depend on pre-patterning of the substrate with different lithography techniques, and they cannot be categorized under the full self-assembly orientation of the BCP, and therefore they are beyond the scope of this report [1].

Table 1: Summary of common methods to orient the micro domains later and/or perpendicular to the substrate surface [1-6].

Interactions	Driving forces	Experimental methods	Characteristics	Type of sample
Mechanical flow fields	Shear and elongation	Extrusion	Easy control, large samples	Bulk
	Shear	Rheometer	Easy control of parameters	Bulk
	Compression	Channel die	Simple apparatus	Bulk
	Shear and elongation	Roll casting	Ordering from solution	Bulk
	Elongation	Petermann method	Semicrystalline BCP	Thin films
Temperature gradient	Temperature gradient	Zone refining cell	High degree of orientation, slow process	Bulk
Electric field	Dielectric contrast	In-plane and vertical	Low degree of orientation lack of lateral orientation	Bulk/thin films
Surface tension	Surface tension	Spreading on a fluid surface	Liquid crystalline/semicrystalline BCP	Thin films
Thickness and substrate	Commensurability	Thickness control	Parallel/vertical LAM, CYL	Thin films
	Preferential wetting	Confinement	Only parallel ordering	
	Neutral substrate	Random copolymer	Vertical LAM, CYL w/o lateral order	
Special block copolymers	Architecture	Spin coating	Vertical LAM w/o lateral order	Thin films
	Liquid crystallization		Vertical LAM w/o lateral order	
	Crystallization and wetting/dewetting		Vertical LAM w lateral order near wet./dewet. boundary	
Solvent control	Evaporation rate	Spin coating	Vertical CYL w slow evap. rate	Thin films
	Prewetting		In-plane CYL near rims	
Patterned substrates	Chemical pattern	Soft lithography	Vertical/parallel LAM	Thin films
		Silicon miscut	Vertical LAM	
		Holographic pattern	Conformal/anticonformal	
	Topographic pattern	Softlithography	Micromolding	
		Chemical/topographic	Silicon miscut/metal deposition	

1.15 PS-b-PMMA Thin Film

We focus on PS-b-PMMA (poly (styrene) and poly (methyl methacrylate)).Figure 8 shows the chemical structure of the PS-b-PMMA block copolymer.

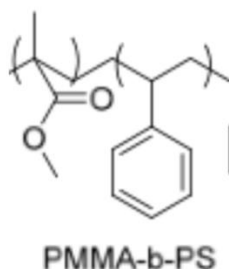


Figure 8: Chemical structure of PMMA-b-PS.

In this study, we used PS-b-PMMA block copolymer for variety of reasons. First of all, PS-b-PMMA is available as commercial BCP. Second, it has narrow molecular weight distributions of each block. Third, PMMA is a standard photoresist and a PS is negative e-beam resisting. Fourth, the surface energies of PS and PMMA are very similar which make it easier to control the orientation of the nano-domains within the film. Lastly, PS-b-PMMA has a small Flory-Huggins interaction parameter (~ 0.043 at 25°C) compared to the other BCPs as shown in table 2. Small Flory-Huggins interaction parameter is bad for high resolution but it is easier to work with.

These properties of PS-b-PMMA make it a great candidate for nanolithography and pattern transfer applications. Thurn-Albrecht et al. [15-1] first reported the application of PS-b-PMMA to fabricate a porous polymer template. In their method, they have treated the PMMA block by exposing it to the UV light, and cross linking the PS block. Further, they developed (removed the PMMA block) the pattern by the use of Acetic Acid, which resulted in a nanoporous template on

top of their substrate.

Table 2: Flory–Huggins parameter for different BCPs [1-15].

polymer name	Flory–Huggins		
	parameter	χ at 25°C	χ at 180°C
PS- <i>b</i> -PMMA [57]	$4.46 T^{-1} + 0.028$	~ 0.043	~ 0.038
PS- <i>b</i> -PEO [58]	$29.8 T^{-1} - 0.023$	~ 0.077	~ 0.043
PS- <i>b</i> -PI [59]	$33 T^{-1} - 0.0228$	~ 0.088	~ 0.050
PS- <i>b</i> -P2VP [60]	$63 T^{-1} - 0.033$	~ 0.178	~ 0.106
PS- <i>b</i> -PLA [61]	$98.1 T^{-1} - 0.112$	~ 0.217	~ 0.105
PS- <i>b</i> -PDMS [58]	$68 T^{-1} + 0.037$	~ 0.265	~ 0.187
PTMSS- <i>b</i> -PLA [62]	$51.3 T^{-1} + 0.29$	~ 0.478	~ 0.403
PS- <i>b</i> -PFS	n.a.	n.a.	n.a.

1.16 Pattern Transfer Method

Isotropy and anisotropy

When a material is attacked by a liquid or vapor etchant, it is removed isotropically (uniformly in all directions) or anisotropic etching (uniformity in vertical direction). The difference between isotropic etching and anisotropic etching is shown in Figure 9. Material removal rate for wet etching is usually faster than the rates for many dry etching processes. The wet etching rate can be varied by varying the temperature or the concentration of active species [18].

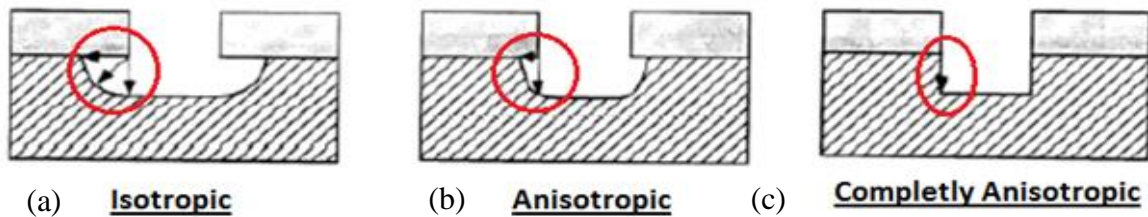


Figure 9: (a) Isotropic etching of silicon (b) Partially anisotropic and (c) Completely anisotropic

1.16.1 Dry Etching

Dry etching is widely used to transfer the pattern through the mask to the substrates. Dry etching is typically used for directional etching. The reaction that takes place can be done utilizing the high kinetic energy of particle beams, chemical reaction or the combination of both [18].

1.16.1.1 Physical Dry Etching

Physical dry etching requires high kinetic energy (ion, electron, or photon) beams to remove the substrate atoms. When the high-energy particles knock out the atoms from the substrate surface, the material evaporates after leaving the substrate. There is no chemical reaction taking place and therefore only the material that is unmasked will be removed [18]. Figure 10 illustrates the physical reaction.

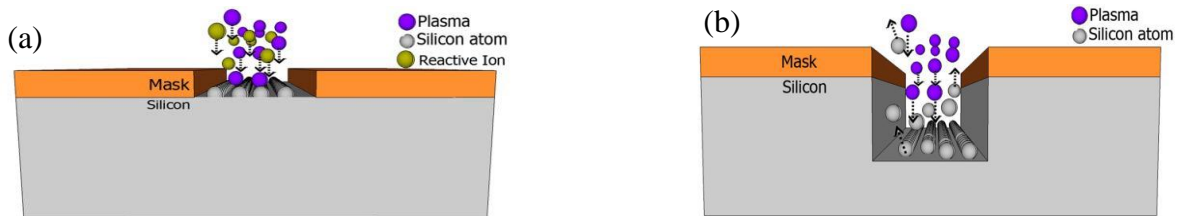


Figure 10: Schematic representing dry etching mechanism. The plasma hits the silicon wafer with high energy to knock-off the Si atoms on the surface. (a) The plasma atoms hitting the surface. (b) The silicon atoms being evaporated off from the surface. [18]

1.16.1.2 Chemical Dry Etching

Chemical dry etching is also called vapor phase etching. This etching process does not

use liquid chemicals or etchants. In this process, a chemical reaction takes place between etchant gases and silicon surface. The chemical dry etching process is usually isotropic and exhibits high selectivity [18]. Anisotropic dry etching has the ability to etch with finer resolution and higher aspect ratio than isotropic etching. Due to the directional nature of dry etching, undercutting can be avoided [18]. Figure 11 shows the reaction that takes place in chemical dry etching. Some of the ions that are used in chemical dry etching are tetrafluoromethane (CF_4), sulfur hexafluoride (SF_6), nitrogen trifluoride (NF_3), chlorine gas (Cl_2), or fluorine (F_2).

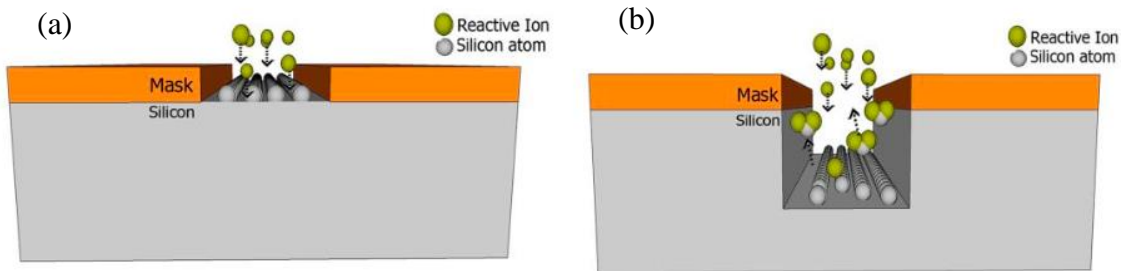


Figure 11: Process of a reactive ion interacting with the silicon surface. (a) The interaction between the reactive ion and the silicon atom. (b) A bond between the reactive ion and the silicon atom then chemically remove the silicon atoms from the surface. [18]

Once the desired morphology is reached on the surface of the substrate, Oxygen plasma is used to selectively remove PMMA component and the underlying films, C_2F_8 and O_2 [19] are used to remove the polymer and finally SF_6 is used to etch the silicon. Figure 12 depicts the pattern transfer of the Lamellae structure into silicon substrate with an under-layer of PS-OH to neutralize the surface. Typically, to achieve periods smaller than 20nm, the thickness of the BCP template must be very small. This film thickness reduction limits the fidelity of the pattern transfer, due to low selectivity in the etching rate of the BCP blocks. Since the selectivity of most BCPs are very close to each other, the fidelity of the transfer can be compromised when the film thickness is low.

To solve the selectivity issue, additional step is introduced in pattern transfer of PS-b-PMMA to stay. Just like the pattern development process in lithography technique, in some cases, aside from the RIE, UV exposure and solvent development is employed to remove PMMA micro-domains from the PS-b-PMMA masking pattern. A film with higher selectivity can also be deposited on top of the PS-b-PMMA masking layer to create a negative replica of the template. Next, the new mask (usually a metal layer) with the negative pattern is used to transfer the pattern into the substrate material. Black et al. [20] showed that PS-b-PMMA block copolymer can be used as an etching mask to pattern transfer using the fluorine (SF_6) Reactive Ion Etching (RIE). For silicon (Si) and metals, fluorine-based etch chemistry, using fluorinated gases such as SF_6 , C_2F_8 or CHF_3 , in combination with argon (Ar) gas, are the most effective [20]. The etch rates depend on the different ionization and acceleration conditions. Typically, a higher RF power increases the ion density, and, consequently, the etch rate. Ion milling, which is physical bombardment of the substrate surface by the ions, is typically uses Ar ions. Ion milling is similar to RIE, but based on a directional sputtering process.

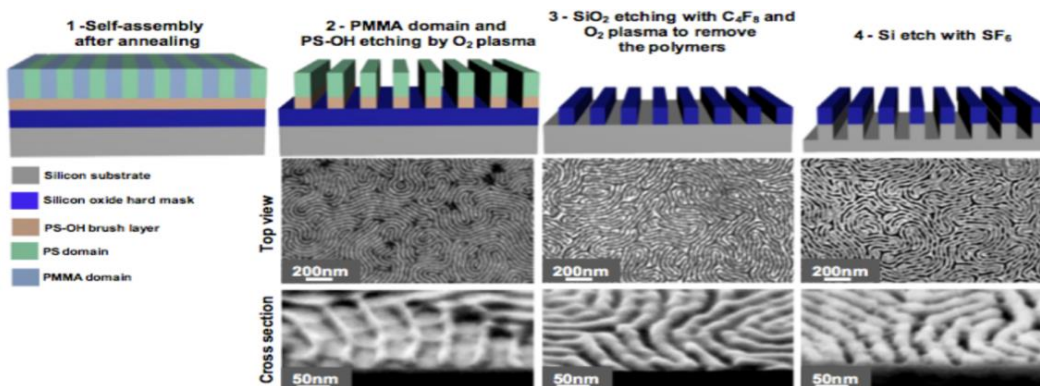


Figure 12: Pattern transfer using the PS-b-PMMA block copolymer as an etching mask

1.16.2 Wet Etching

The principle of wet etching is similar to dry etching, but to remove the material from the wafer, the etching process uses a liquid medium. The specific patterns are defined by masks on the wafer. Materials that are not protected by the masks are removed away by liquid chemicals. These masks are deposited and patterned on the wafer in a prior fabrication step using lithography. A wet etching process involves different chemical reactions which consume the original reactants and produce new reactants. The wet etching process consist of three main steps: (1) Diffusion of the liquid etchant to the structure that is to be removed. (2) The reaction between the liquid etchant and the material being removed away. A reduction-oxidation (redox) reaction usually occurs. This reaction requires the oxidation of the material then dissolving the oxidized material. (3) Diffusion of the byproducts in the reaction from the reacted surface [18].

1.16.2.1 Anisotropic Wet Etching

At different rates, liquid etchants etch crystalline materials depending upon which crystal face is exposed to the etchant. There is a huge difference in the etch rate depending on the silicon crystalline plane. In such materials as silicon, this effect can allow for very high anisotropy. Some of the anisotropic wet etching agents for silicon are potassium hydroxide (KOH), ethylenediamine pyrocatechol (EDP), or tetramethylammonium hydroxide (TMAH). Etching a (100) silicon wafer would result in a pyramid shaped etch pit as shown in Figure 13a. The etched wall will be flat and angled. The angle to the surface of the wafer is 54.7° . Figure 13c-d shows scanning electron micrographs of (110)-oriented two-dimensional silicon walls with micro and nanoscale dimensions generated based on KOH wet etching.

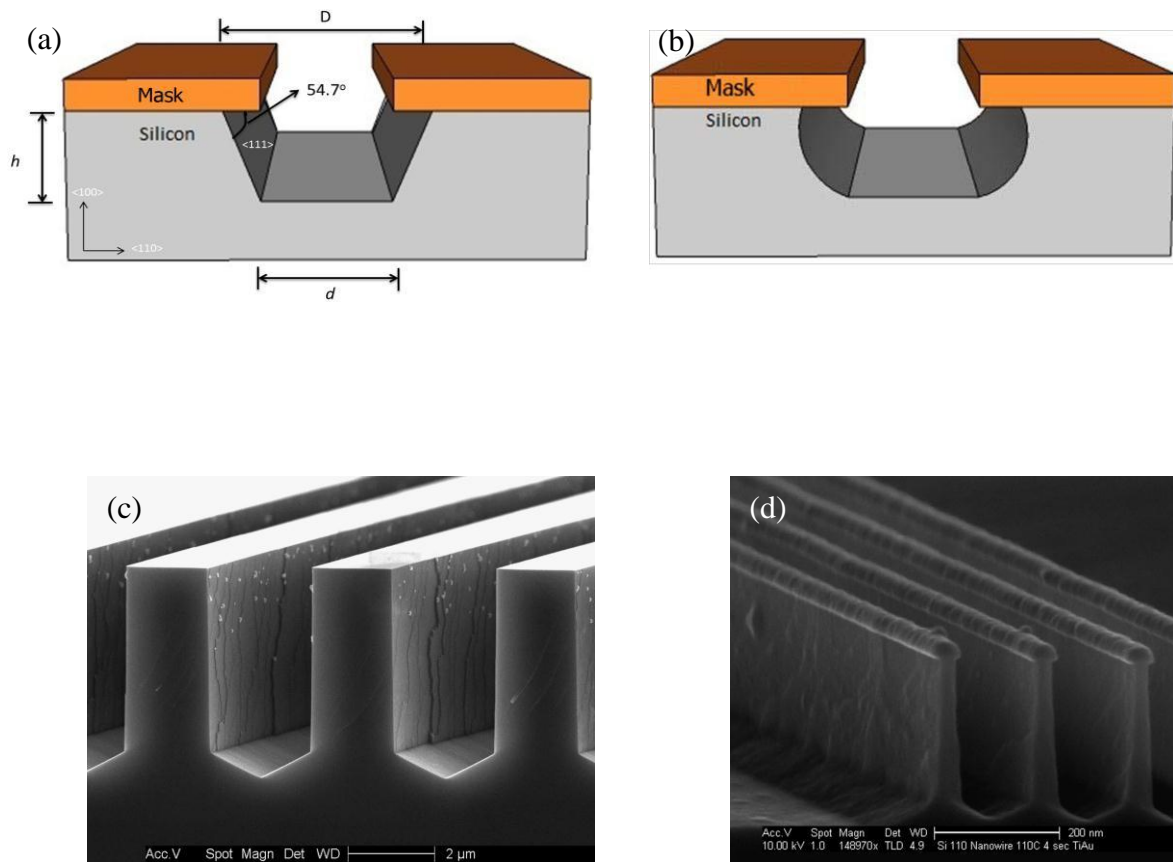


Figure 13: Schematics of an etch profile in (a) an anisotropic and (b) an isotropic etch of a (100) oriented silicon surface. (c, d) KOH based wet etching of (110)-oriented Si surfaces with micro and nanoscale two-dimensional walls. [18]

1.16.2.2 Isotropic Wet Etching

A mixture of hydrofluoric acid (HF), nitric acid (HNO₃) and acetic acid (HNA) is the most common etchant solvent for silicon. The concentration of each etchant determines the etch rate. Either silicon dioxide or silicon nitride is usually used as a masking material against HNA. When the reaction takes place, the material is removed laterally at a rate similar to the speed of downward etching. The lateral and downward etching process takes places even with isotropic dry etching as

described in the dry etching section. Wet chemical etching is generally isotropic even though a mask is present since the liquid etchant can penetrate underneath the mask (Figure 13.b). When the direction is very important for high-resolution pattern transfer, wet chemical etching is normally not used [18].

1.17 Conclusion

Semiconductor industry is converging on a limit to the Moore's Law due to the limitation on current method of lithography. Thus, a revolutionary approach is in demand to further help the industry to meet the fast-growing technological world. One of the currently studied methods is block copolymer self-assembly. Due to its interesting features and its ability to arrange into nanometer structure, self-assembled block copolymer has high potential in the semiconductors industry. In fact, poly(styrene)-b-poly(methyl methacrylate) (PS-b-PMMA) is commonly linked to "bottom-up" method of fabrication due to the fact that it can be controlled by altering the surface energy of the substrate. Several methods were developed to tune the substrate's surface energy; however, due to the possibility of contamination and the difficulty of scaling them, they are not optimal for industry.

Chapter 2. Experimental Work and Results

2.1 Introduction

Block copolymer lithography holds a great potential for applications in nanofabrication due to its ability to self-assemble into periodic structure on the tens of nanometer length scale. As discussed in the previous chapter, the size and morphology of the self-assembled nano-domain is controlled by the molecular weight and composition of the BCP. Therefore, the use of block copolymer lithography to achieve nano-structures over a large area, along with other nanofabrication techniques, is relatively easy. This chapter discusses the procedures and the tools that were used to obtain a perpendicular lamellae structure. Furthermore, the effect of changing annealing time on the lamellar forming BCP of PS-b-PMMA was studied as well.

2.2 Preparation Of PS-b-PMMA Film

In this experiment, various molecular weight of PS-b-PMMA solvent manufactured by Advanced Polymer Materials Inc. were used. The molecular weights used were (65.3-66.6, 32.5-39.6, and 19.1-19.2) kg/mol. The solution was prepared by mixing BCP in 1% toluene.

2.3 Deposition Of Aluminum On Top Of The Silicon Wafer

An 8nm Al layer was deposited onto the bare silicon wafer by e-beam evaporator. After that, few samples were cut into $1 \times 1 \text{ cm}^2$ squares. Those samples were cleaned by acetone and isopropanol and dried with nitrogen. To clean any organic contaminate, oxygen plasma treatment

was used. The parameters of oxygen plasma were 20 mTorr pressure, 20 W RF power, and 20 sccm O₂ flow for 60 seconds.

2.4 Coating PS-b-PMMA BCP Thin Film With A Surface Neutralizing Underlayer

B.H. Sohn and S.H. Yum [21] first discovered the use of 3-(p-methoxyphenyl) propyltrichlorosilane (3-MPTS) monolayer to reduce the surface energy of the substrate to produce upright lamellar morphology for the PS-b-PMMA BCP [21]. To get very well defined and perpendicular micro-domains, they coated the 3MPTS monolayer first, then the BCP. Their method produced very good results. However, the coating process was long and took almost 48hours [21]. This long time cannot be acceptable for high throughput fabrication.

The coating process were done twice in the present work. We modified the B.H Sohn and S.H. Yum's method to obtain perpendicular lamellar morphology. Before coating the BCP, multiple drops of 3-(p-methoxy phenyl) propyl trichloro silane (MPTS) by Gelest Inc. were added inside wafer box that had the cleaned Si on the top of wafer cap without allowing the substrate to touch the droplets.

As shown in figure 14, 3MPTS has both phenyl and O groups. The phenyl group tends to wet the polystyrene, (figure 15), and the O group tends to wet the PMMA.

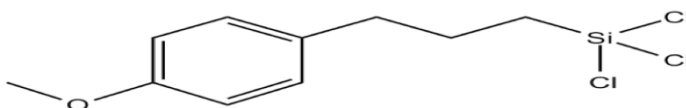


Figure 14: A schematic of the chemical structure of 3-(p-methoxy phenyl) propyl trichloro silane (3-MPTS)

Chemical reaction a shown below:

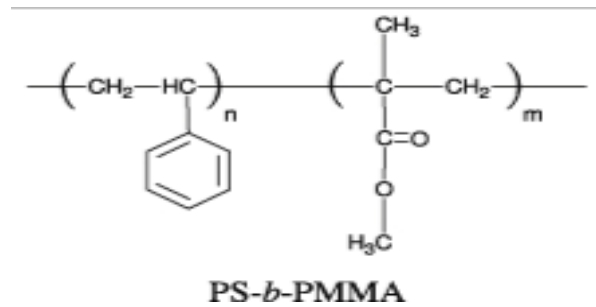


Figure 15: Schematic of PS-*b*-PMMA BCP.

The vapor phase deposition was done for 40 minutes to two hours at room temperature with no vacuum. After the deposition is done, the samples were dipped in acetone for 5 seconds and then in isopropanol for almost 10 seconds to remove any excess MPTS.

PS-*b*-PMMA block co-polymer was spin coated on the Si samples coated with AL then treated with 3MPTS at 2000 rpm for 40 s and the thickness of polymer film was 30-40 nm. To drive off the solvent, the samples were pre-heated at 90 °C for 3 minutes. Under nitrogen environment, the samples were annealed at 190 °C for different times to achieve block copolymer self-assembly structure. After that, oxygen reactive ion etching (RIE) was used to remove PMMA and leave PS. Half of the samples were covered to obtain two areas of dark and bright. The parameters of oxygen reactive ion etching were 10 s at 20 W RF power, 20 sccm O₂ flow and 1

mTorr pressure, with the low pressure giving more anisotropic etching.

The structure characterization was carried out using atomic force microscope (AFM, Bruker Dimension 3100), and scanning electron microscope (SEM, LEO 1530).

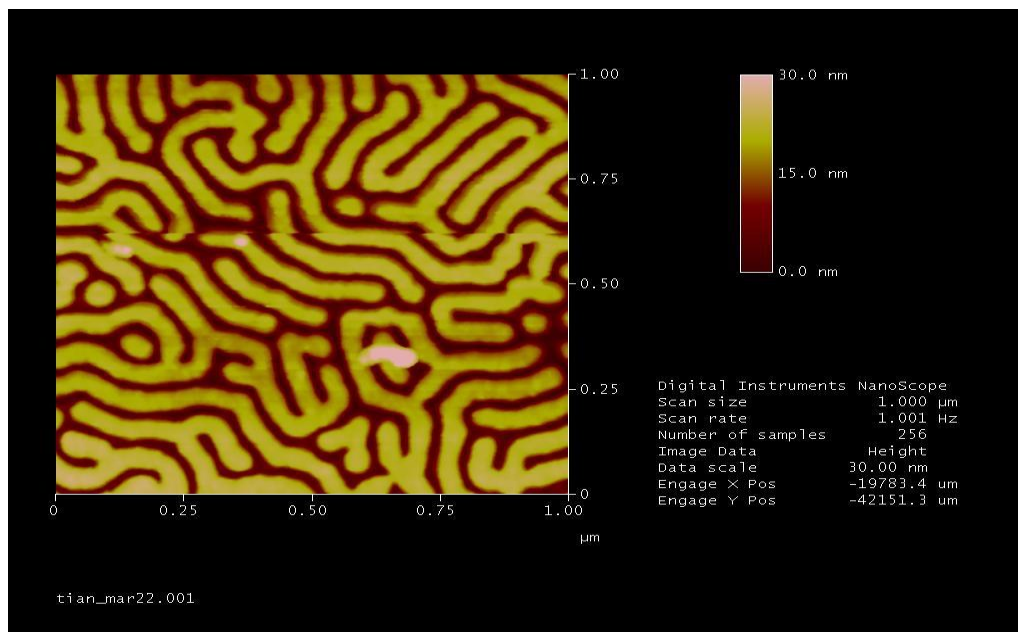


Figure 16: AFM image of self-assembly on PS-b-PMMA after 3MPTS treatment

Figure 16 shows the self-assembly of block copolymer on silicon substrate after a 3MPTS treatment. As it was expected, finger print pattern of the block copolymer is visible in this image. This confirms the successful coating of the 3MPTS monolayer.

It was very challenging task to obtain a smooth SAM of 3MPTS over an entire wafer. If the time and the distance between the drops and the substrate are not favorable, the SAM of 3MPTS will not uniformly cover the substrate surface. This non-uniform coating of the substrate leads to formation of the islands (patches) of lamellar structures as shown in figure 17.

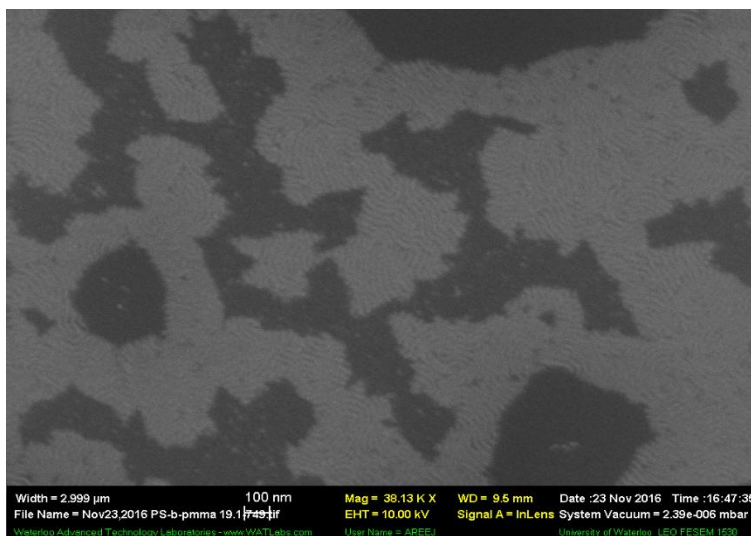


Figure 17: SEM image of the self-assembled of BCP with low coverage of 3MPTS

Optical microscopy was used after each step to check the uniformity of the film. Figure 18 shows the non-uniformity of the film.

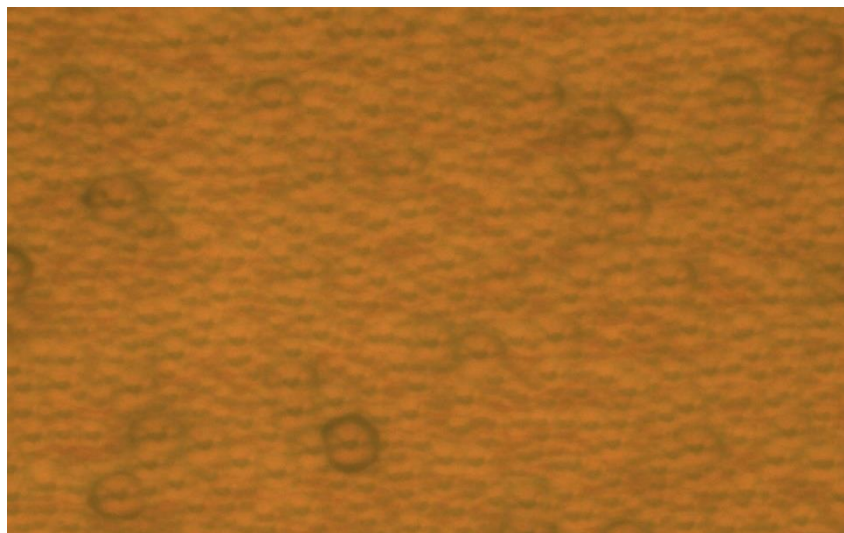


Figure 18: optical microscopy image of thin film after annealing.

To achieve the uniform coating of the substrate with the 3MPTS monolayer, the experimental setup was modified by placing the wafer directly above the 3MPTS droplets. Also, the volume of the droplets under the substrate were decreased. In order to avoid any excess of MPTS which

makes the wafer foggy, we decreased the time to 40 minutes. The process was repeated until a uniform coverage of 3MPTS and BCP was observed as shown in figure 19.

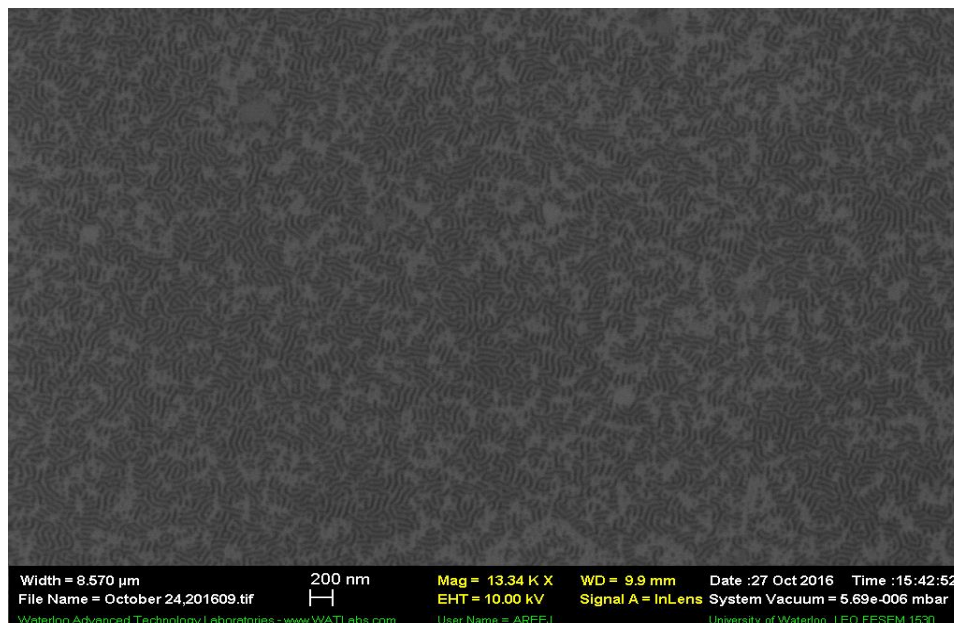


Figure 19: SEM image of the self-assembled of BCP with high coverage of 3MPTS.

After being satisfied with results, we took the optimization process a little further to study the effects of varying the annealing time on the formation of the lamellae micro-domains.

2.5 Varying Annealing Time To Form Self-assembly Of Block Copolymer

Various times were used to study the effect of the annealing time on the formation of lamellae. The same procedure discussed in previous section was used to coat 3MPTS and the same process was used to coat block copolymer on the top of 3MPTS. However, we kept annealing temperature constant at 190 °C while the annealing time was varied between 20 minutes, 1 hour, and 3 hours. The process was followed by oxygen plasma etching to detect the final block co-polymer

morphologies. After that, SEM and AFM were taken to compare the results. Figure 20 to figure 26 show a clear finger print for these annealing times.

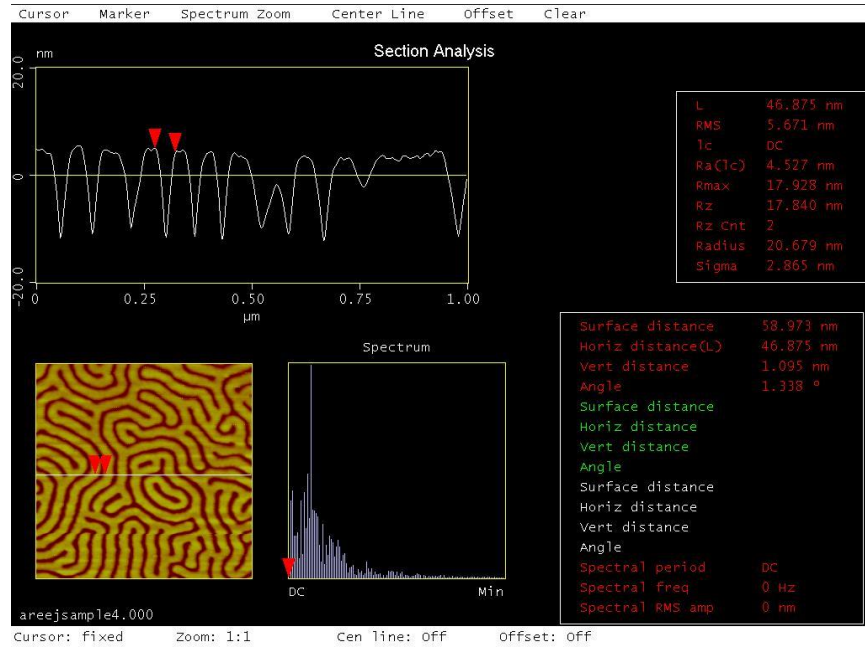


Figure 20: AFM image of annealed BCP at 190 °C for 20 min.

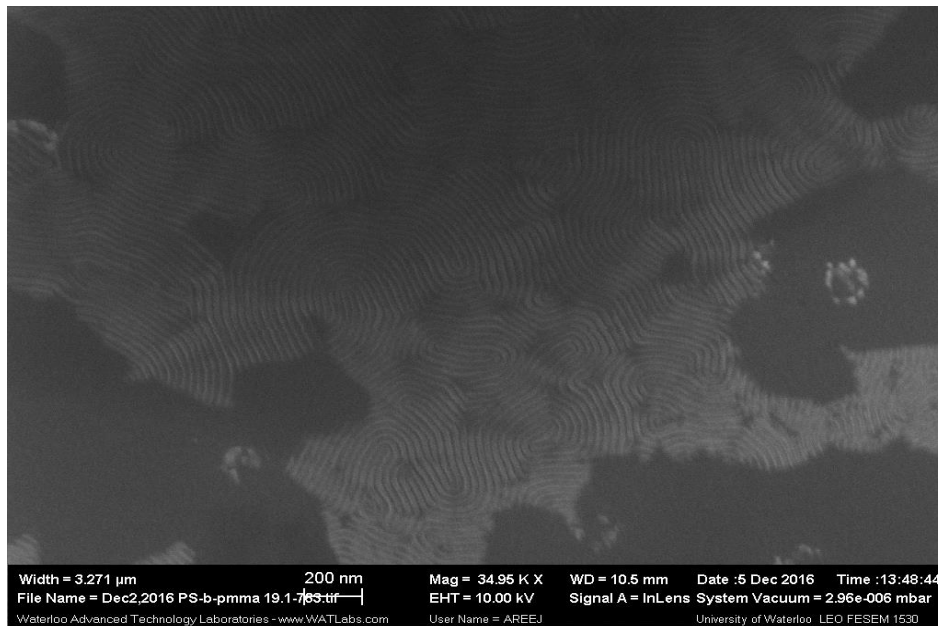


Figure 21: SEM image of annealed BCP 19.1 at 190 °C for 20 min.

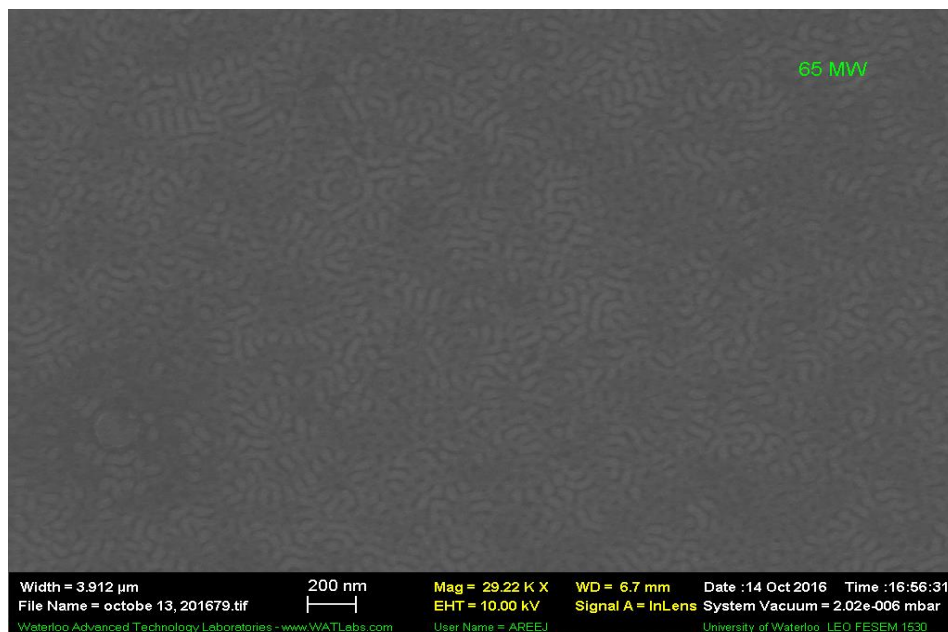


Figure 22: SEM image of annealed BCP 65.6 kg/mol at 190 °C for 20 min.

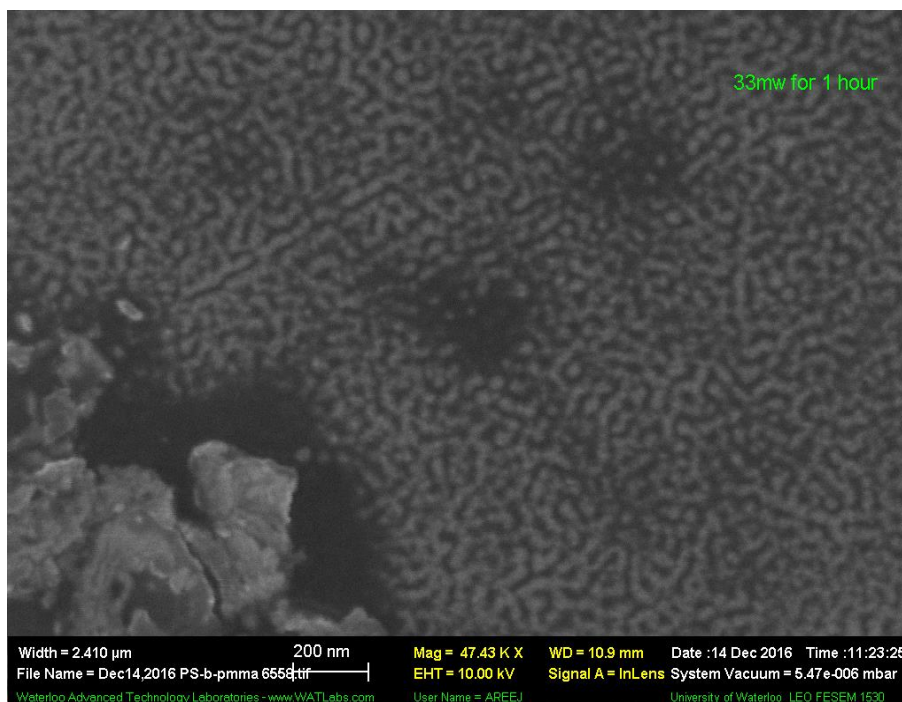


Figure 23: SEM image of annealed BCP 33kg/mol at 190 °C for 1 hour.

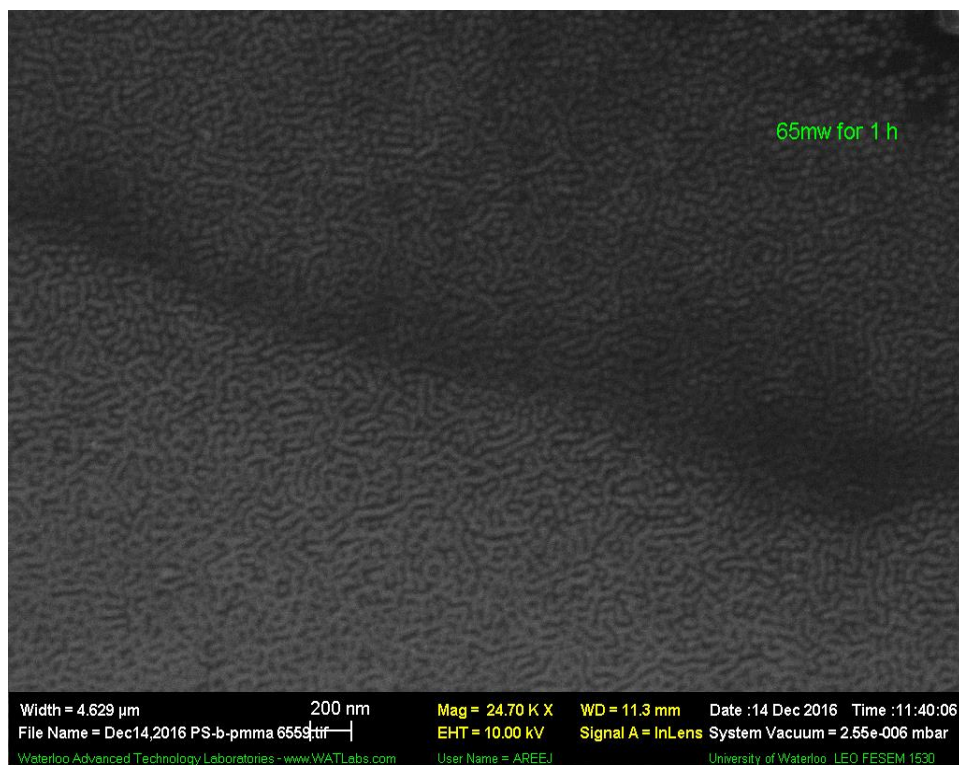


Figure 24: SEM image of annealed BCP 65kg/mol at 190 °C for 1 hour.

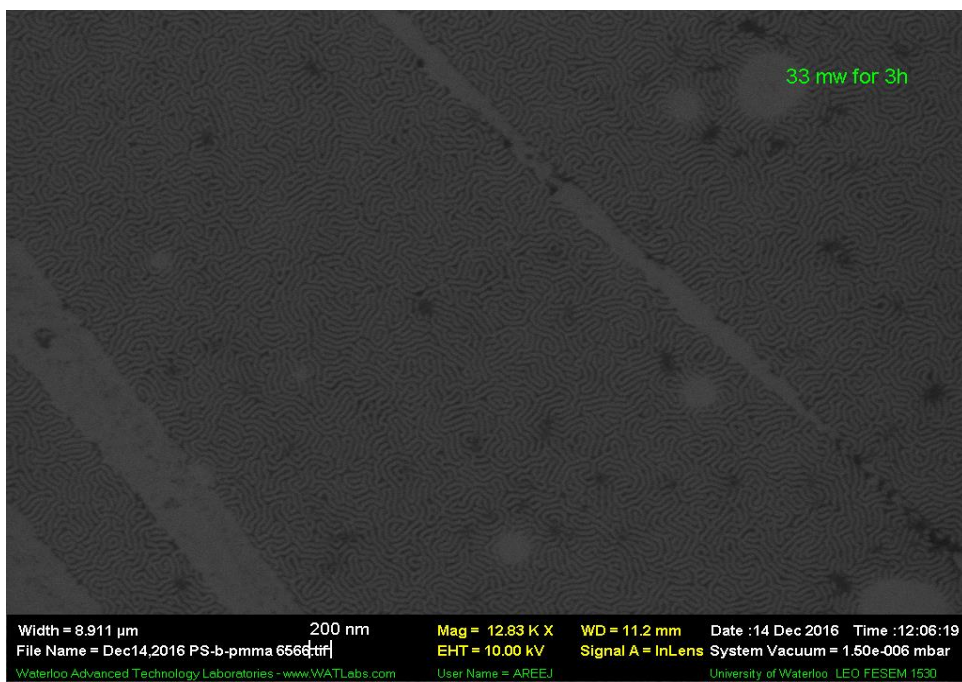


Figure 25: SEM image of annealed BCP 33kg/mol at 190 °C for 3 hours.



Figure 26: SEM image of annealed BCP 65 at 190 °C for 3 hours.

Holes shown in some figures could be due to one of these flowing reasons: the film was too thick, or the film was non-uniform, the annealing time was too short.

2.6 The Effect Of The Soaking Time

Alternative to the simple pattern transfer method using plasma etching that etches the PMMA blocks faster than the PS blocks, we proposed a novel method using wet chemical etching that is of much lower cost than the plasma etching process. As shown in the 27 A, we used an intermediate hard mask layer Al for the pattern transfer. After annealing to induce phase separation, the BCP film is soaked in acetic acid (HAC) that dissolves PMMA without attack of PS. However, the PMMA won't be dissolved and etched away because its chain is bonded to the PS chain. Instead, the PMMA would be displaced, leaving behind some narrow trenches to allow the following

etchant to get through. Afterwards, the sample is rinsed with water and without drying off, the samples were dipped into a solution of HF: acetic acid = 1:3 mixture. The acid mixture would go through the loose trenches and etch the Al underneath, with minimal attack to the Al protected by the PS block. As such, the fingerprint pattern is transferred into the Al. Next, the BCP polymer was etched away by oxygen plasma, and the pattern is subsequently transferred into the underneath silico using F-based etching gas with Al structure as a hard mask. The etching recipe for BCP etching was under 20 Watt RF power, 20 mTorr pressure, and 20 sccm O₂ gas flow for 1 minute, and second to CF₄ for also 1 minute under 20 Watt RF power, 50 mTorr pressure, and 20 sccm gas flow and oxygen gas 4 sccm for Si etching.

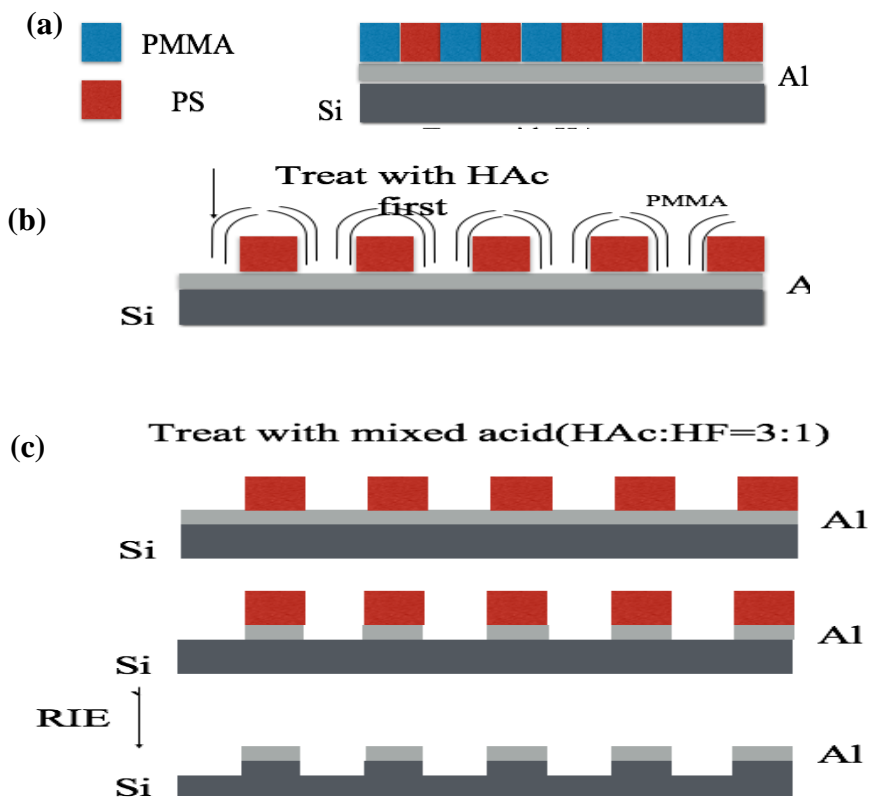


Figure 27: A) schematic of self-assembled lamella on silicon surface. B) After treat with HAC. C) After treated with mixed acid and RIE.

To check if the samples have obtained block co-polymer self-assembly, we cut the dark area of the samples to small pieces and washed the samples by acetic acid for almost 1 minute without drying them. We prepared a 3:1 mixed acid (hydrophobic acid and acetic acid) to soak the samples at different times from 7 seconds to 40 minutes and washed the samples with DI water and dried them. Either AFM or SEM was used to see the characterization of the structure and the results are shown in figs 28-38 for the variable soaking time.

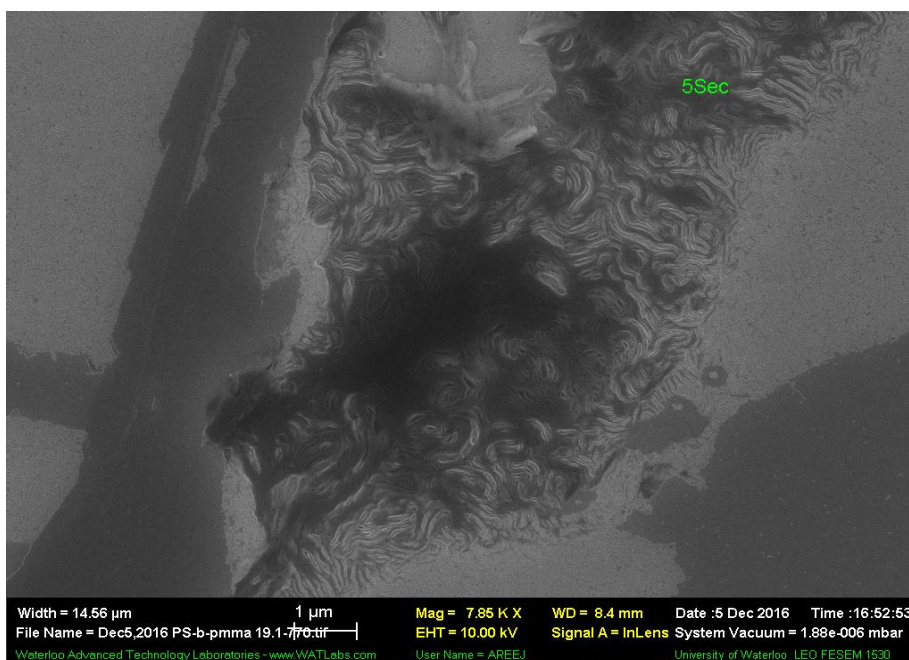


Figure 28: Ps-b-PMMA 19.1 kg/mol after 5 seconds soaking.

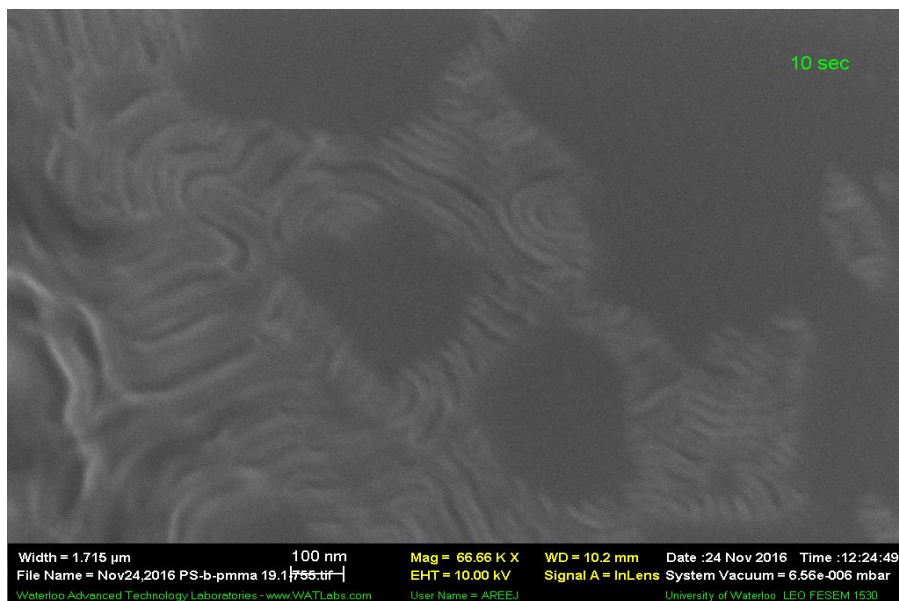


Figure 29: Ps-b-PMMA 19.1 kg/mol after 10 seconds soaking.

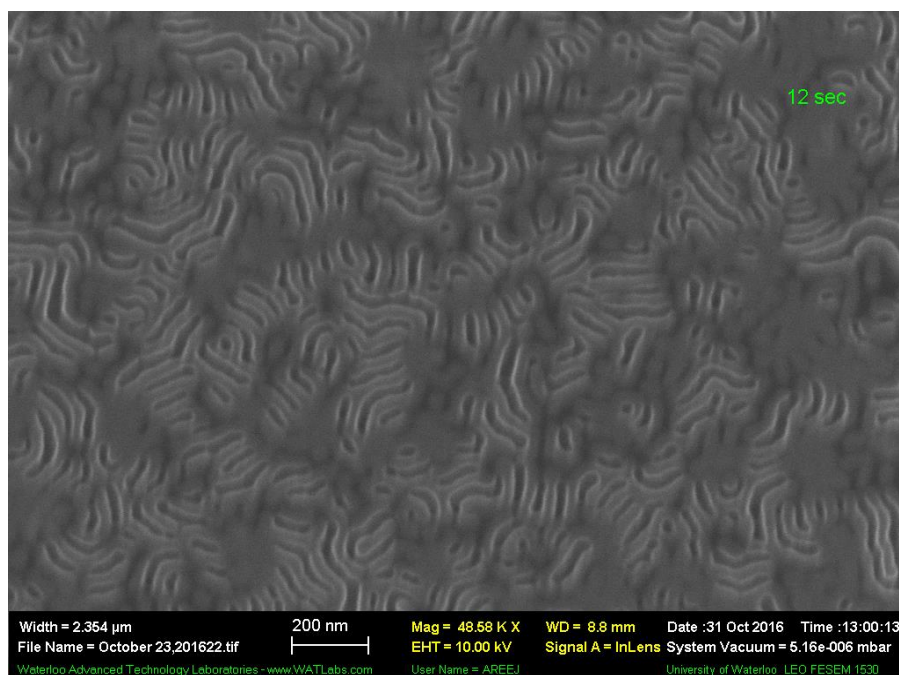


Figure 30: Ps-b-PMMA 19.1 kg/mol after 12 seconds soaking.

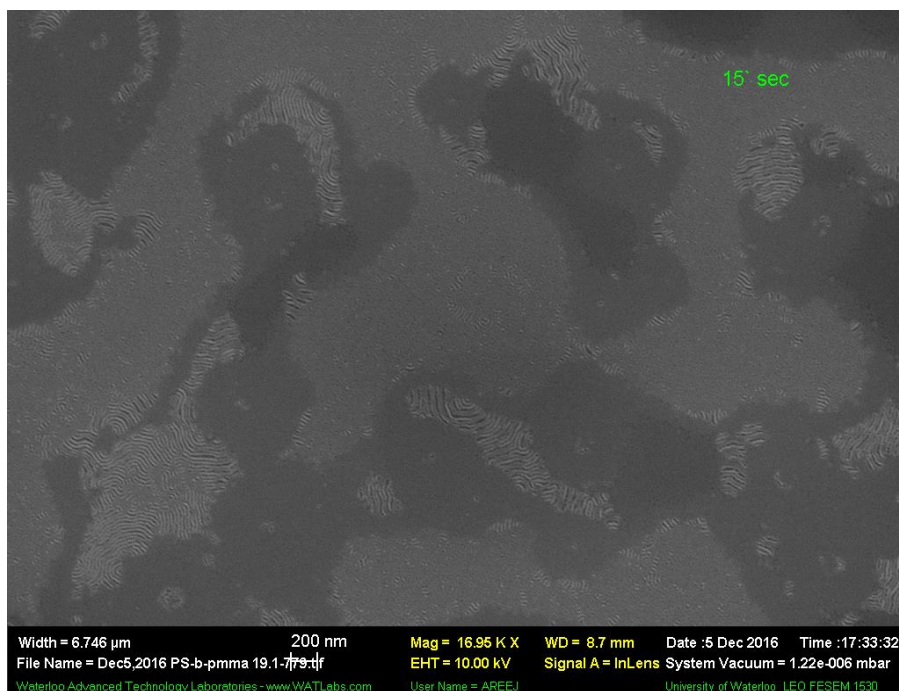


Figure 31: Ps-b-PMMA 19.1 kg/mol after 15 seconds soaking.

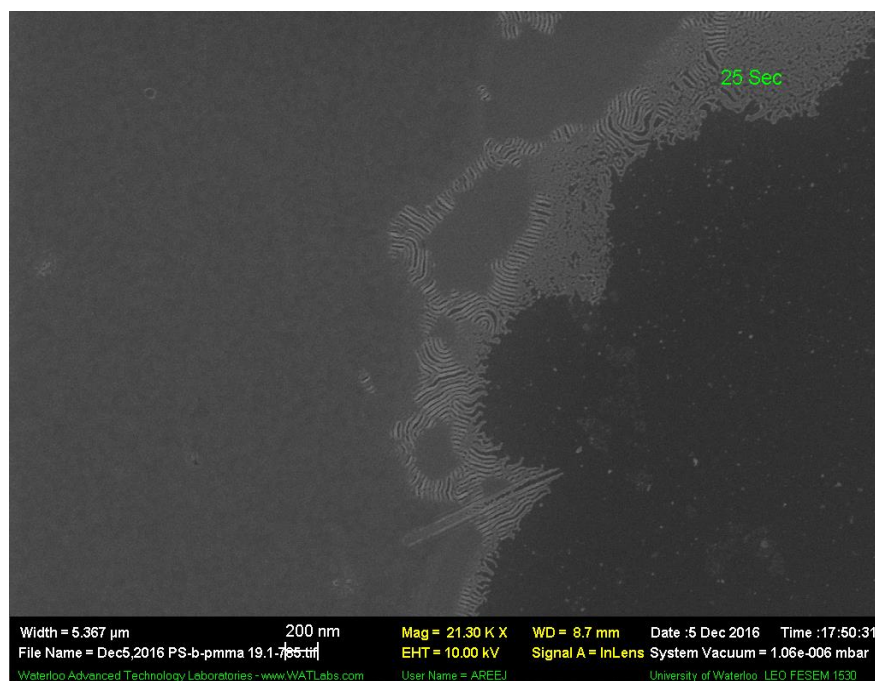


Figure 32: Ps-b-PMMA 19.1 kg/mol after 25 seconds soaking.

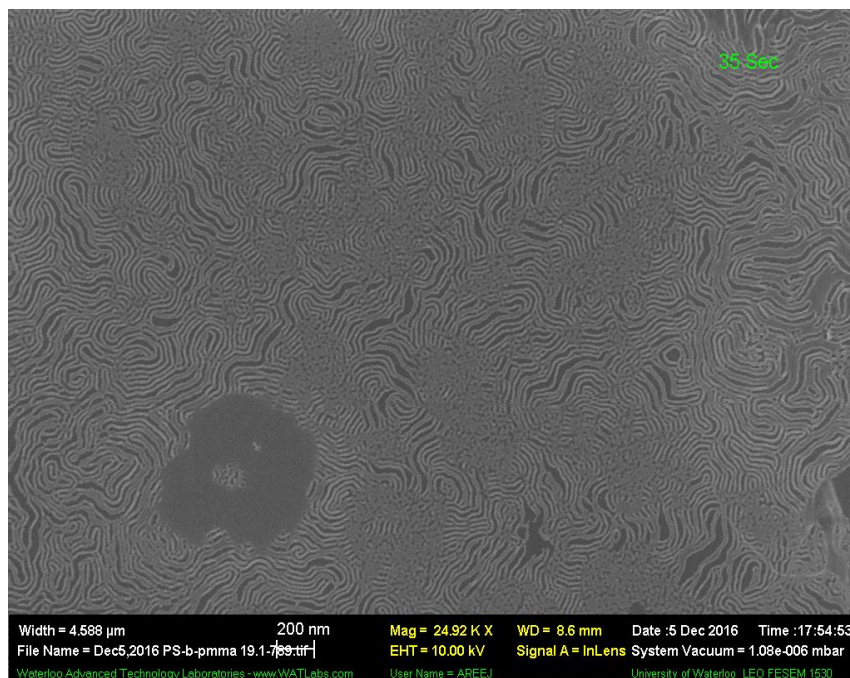


Figure 33: Ps-b-PMMA 19.1 kg/mol after 35 seconds soaking.

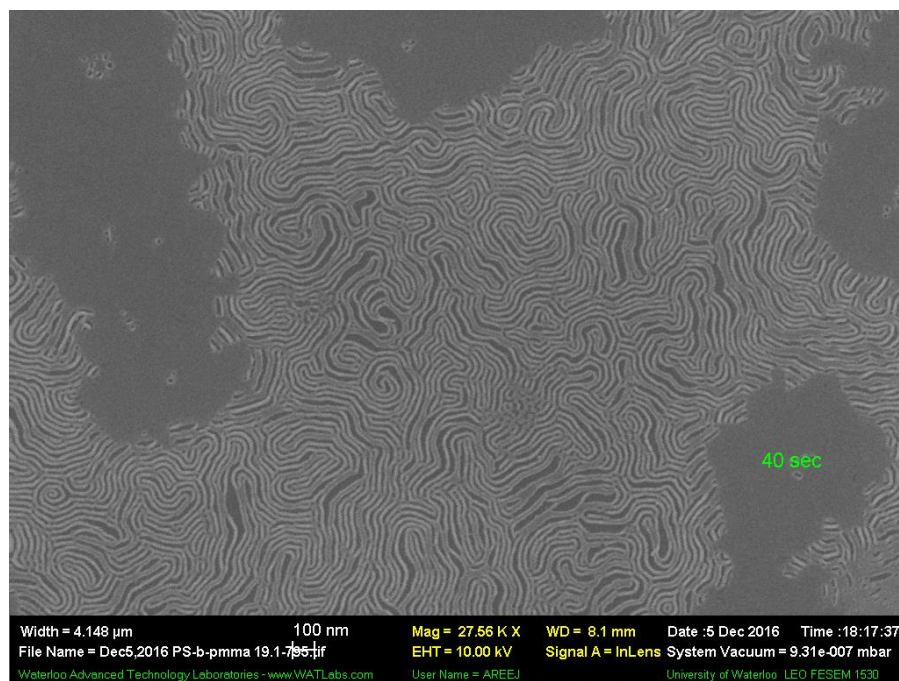


Figure 34: Ps-b-PMMA 19.1 kg/mol after 40 seconds soaking.

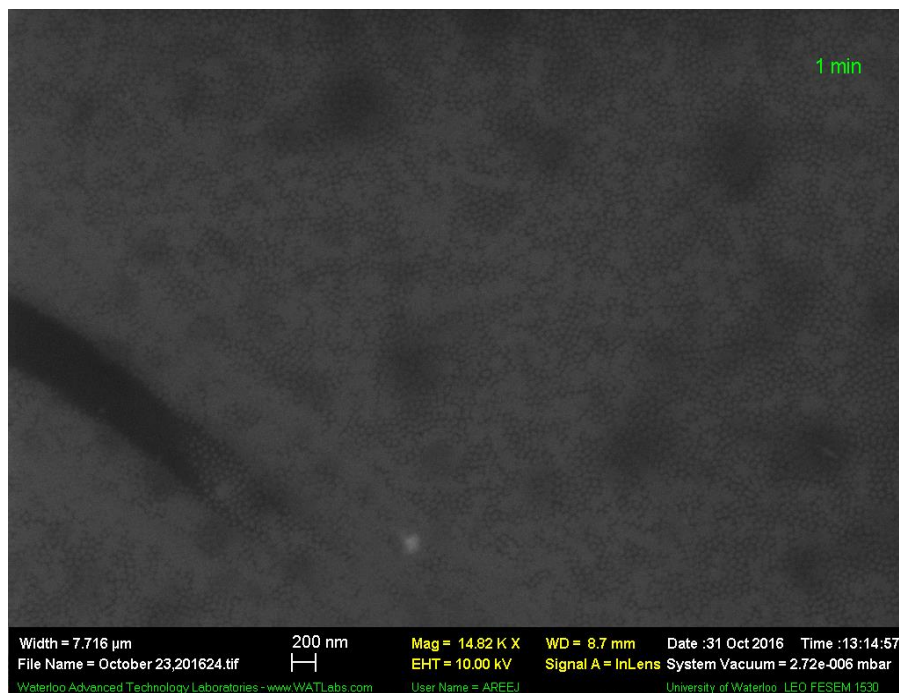


Figure 35: Ps-b-PMMA 19.1 kg/mol after 60 seconds soaking.

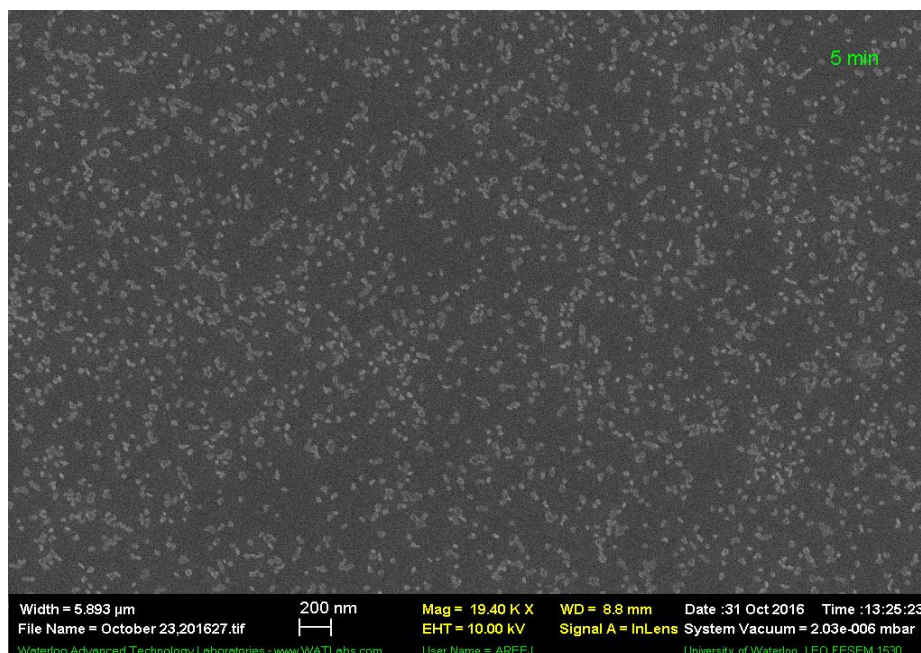


Figure 36: Ps-b-PMMA 19.1 kg/mol after 5 minutes soaking.

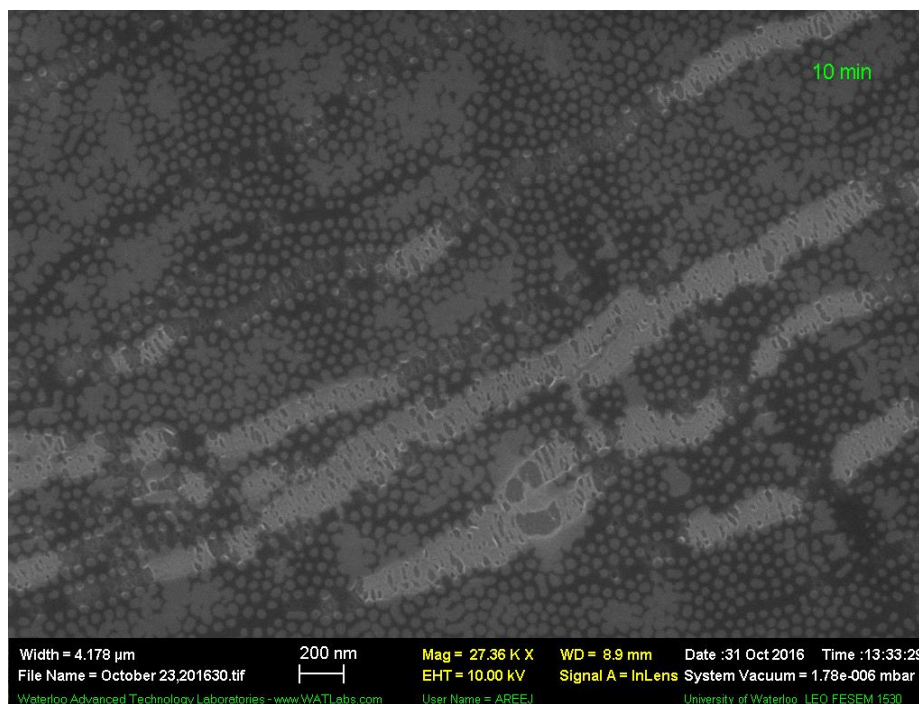


Figure 37: Ps-b-PMMA 19.1 kg/mol after 10 minutes soaking.

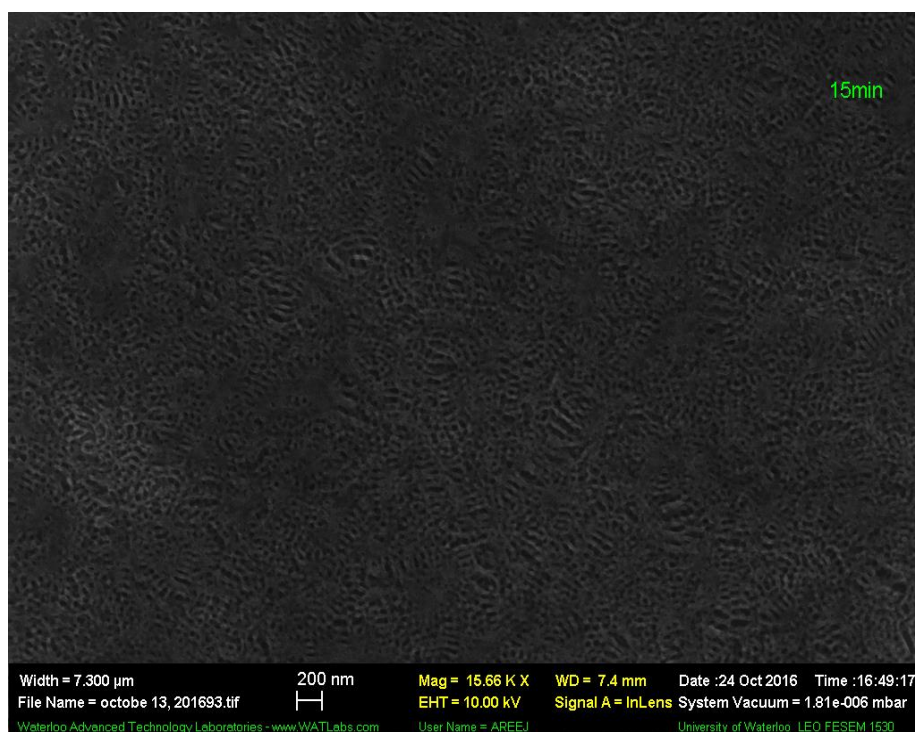


Figure 38: Ps-b-PMMA 19.1 kg/mol after 15 minutes soaking.

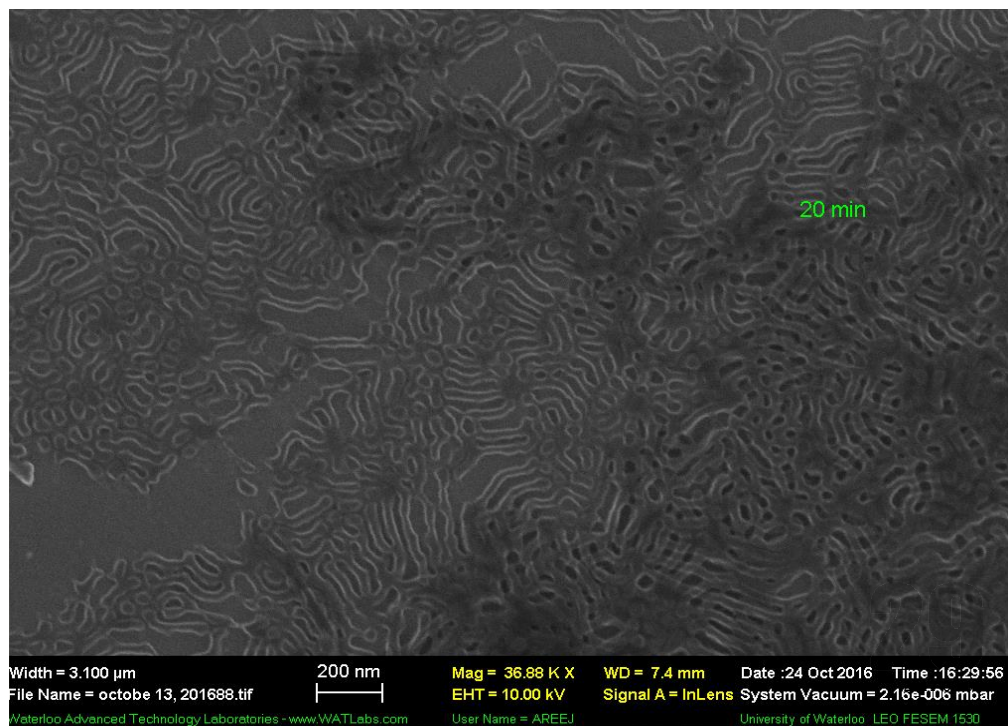


Figure 39: Ps-b-PMMA 19.1 kg/mol after 20 minutes soaking.

Lastly, we used RIE to check if the structure is transferred to silicon through aluminum by the exposure of the block co-polymer to two kinds of gases. First oxygen plasma for 1 minute under 20 Watt RF power, 20 mTorr pressure, and 20 sccm O₂ gas, flow and second to CF₄ for 1 minute under 20 W RF power, 50 mTorr pressure, and 20 sccm gas flow and oxygen gas of 4 sccm. Either AFM or SEM was used to visualize CF₄ the structure and the results are shown in figs 40-52.

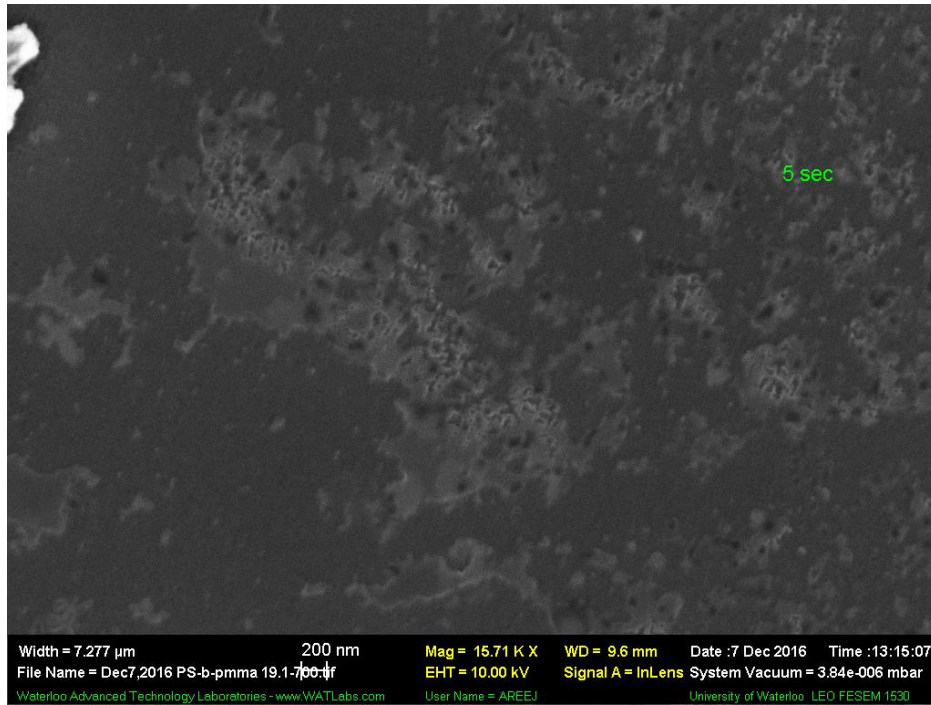


Figure 40: SEM image of etched is structure after RIE (treated time 5 seconds)



Figure 41: SEM image of etched is structure after RIE (treated time 5 seconds).

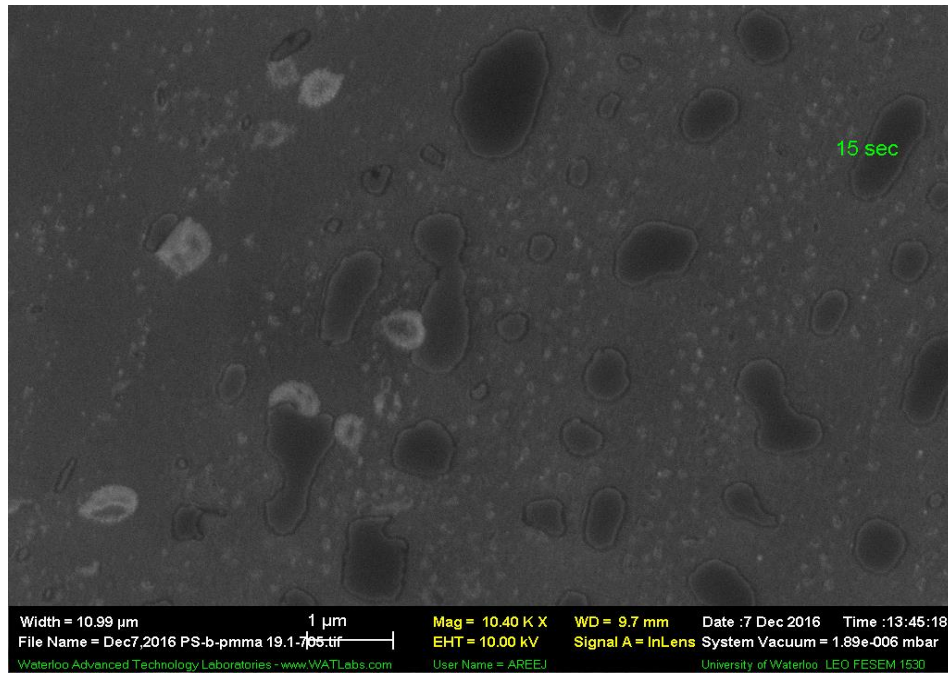


Figure 42: SEM image of etched is structure after RIE (treated time 15 seconds).

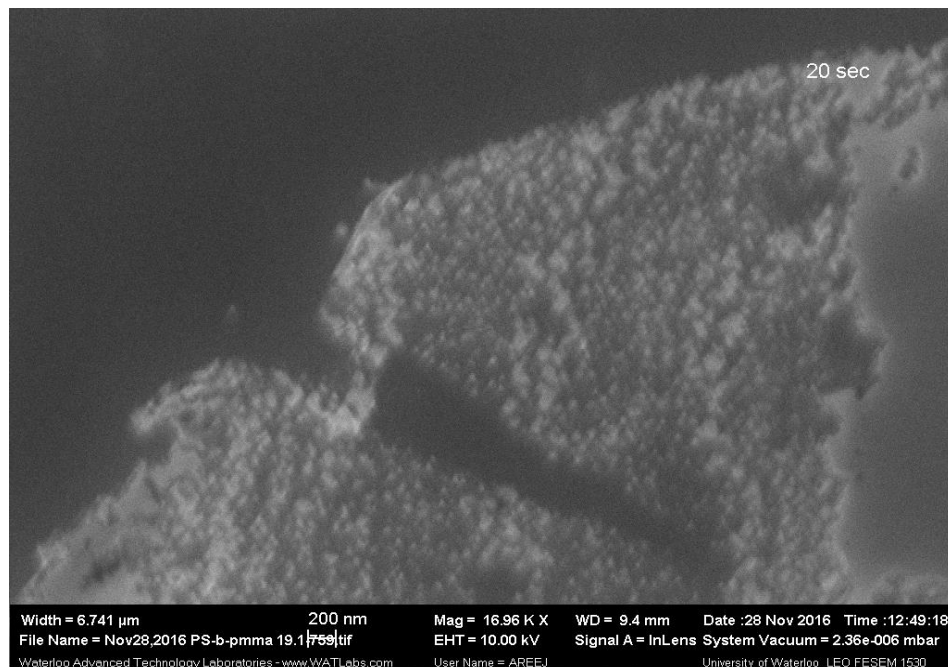


Figure 43: SEM image of etched is structure after RIE (treated time 20 seconds).

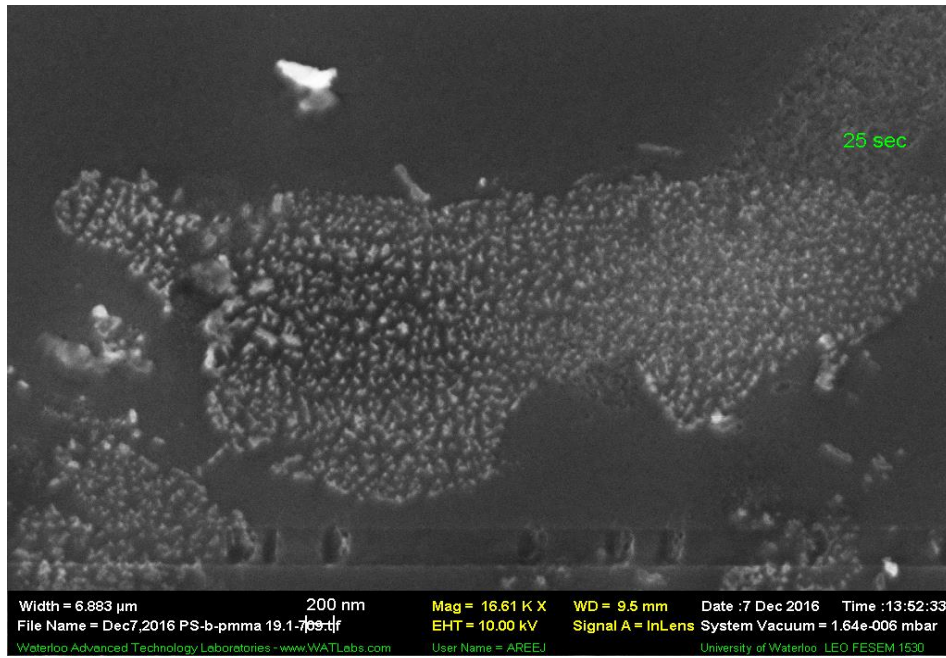


Figure 44: SEM image of etched is structure after RIE (treated time 25 seconds).

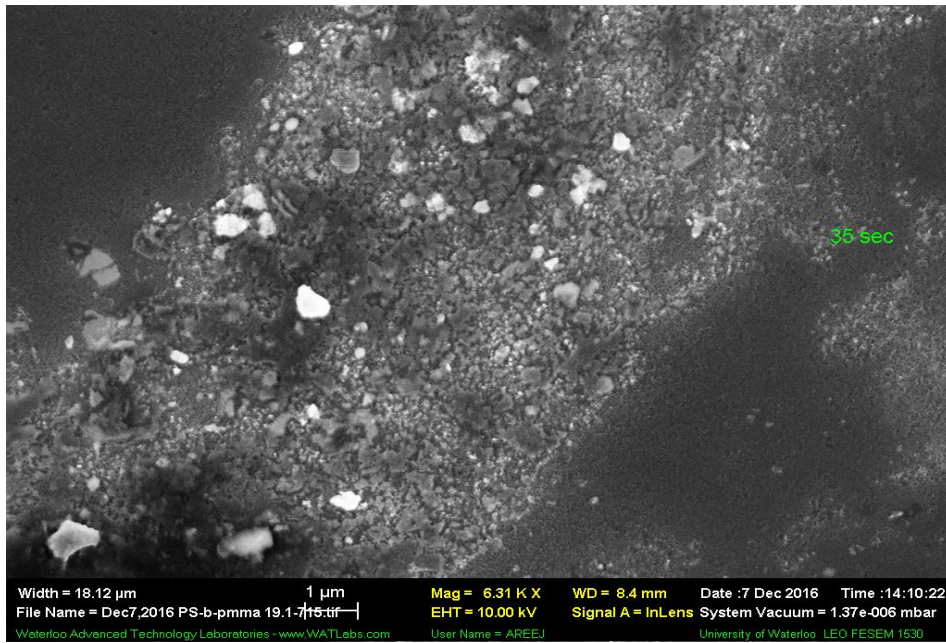


Figure 45: SEM image of etched is structure after RIE (treated time 35 seconds).

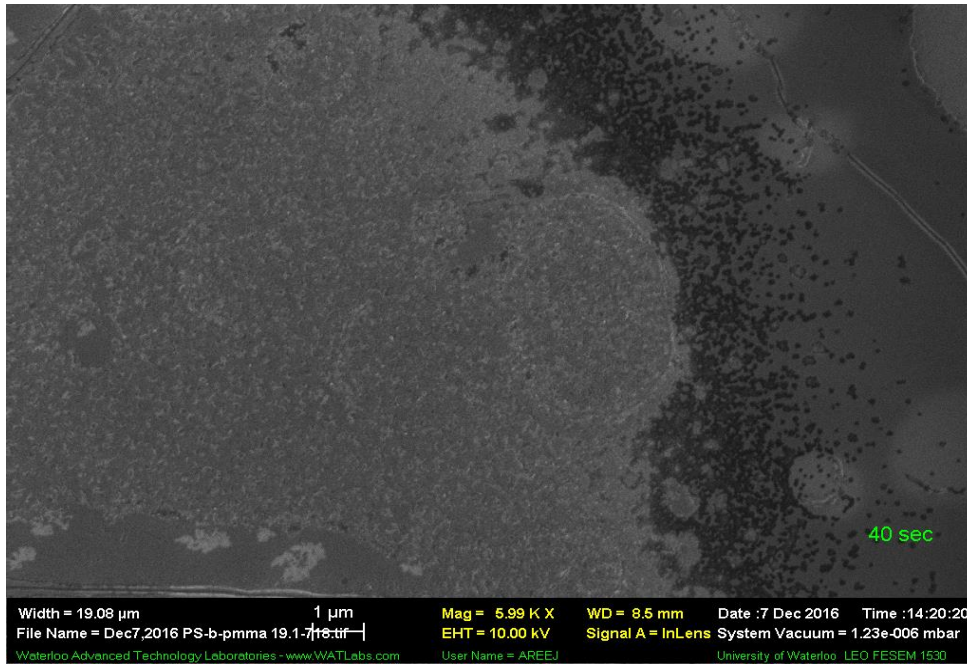


Figure 46: SEM image of etched is structure after RIE (treated time 40 seconds).

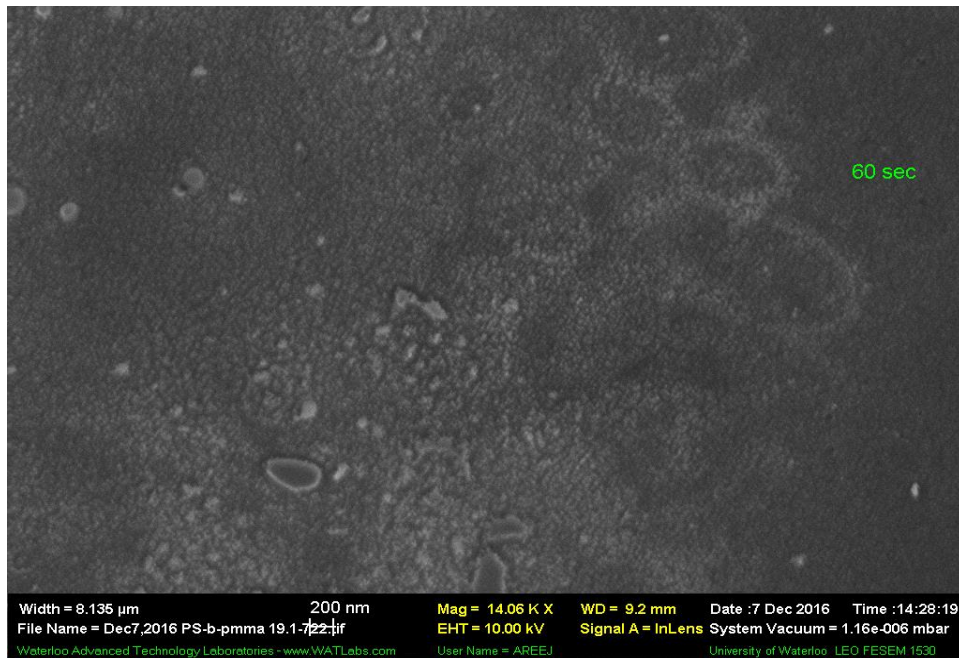


Figure 47: SEM image of etched is structure after RIE (treated time 60 seconds).

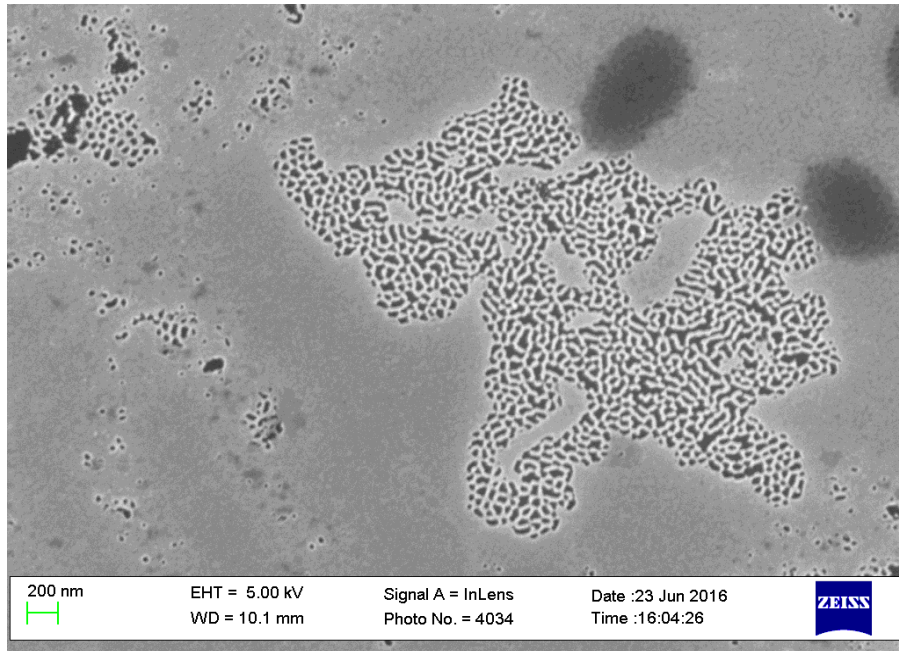


Figure 48: SEM image of etched is structure after RIE (treated time 10 minutes).

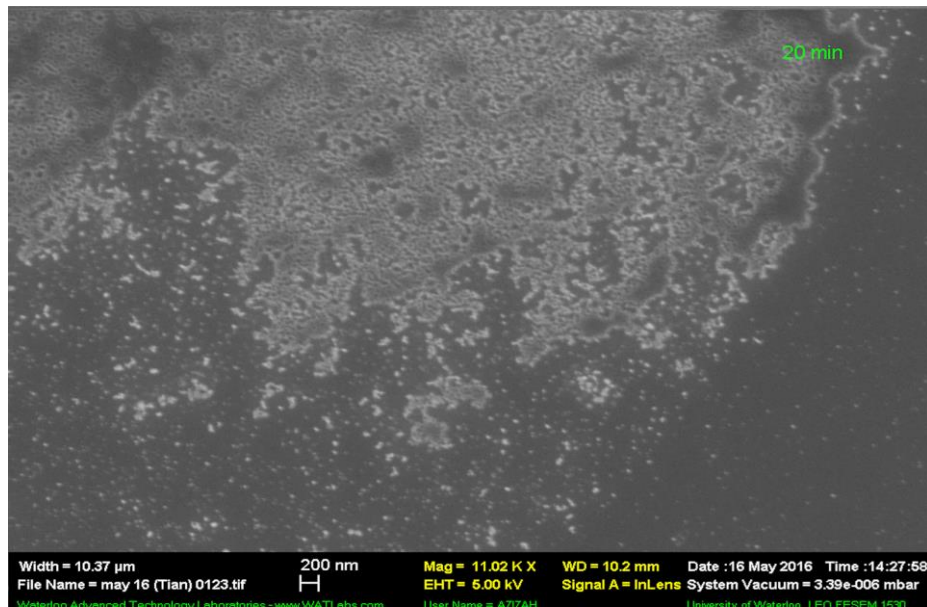


Figure 49: SEM image of etched is structure after RIE (treated time 20 minutes).

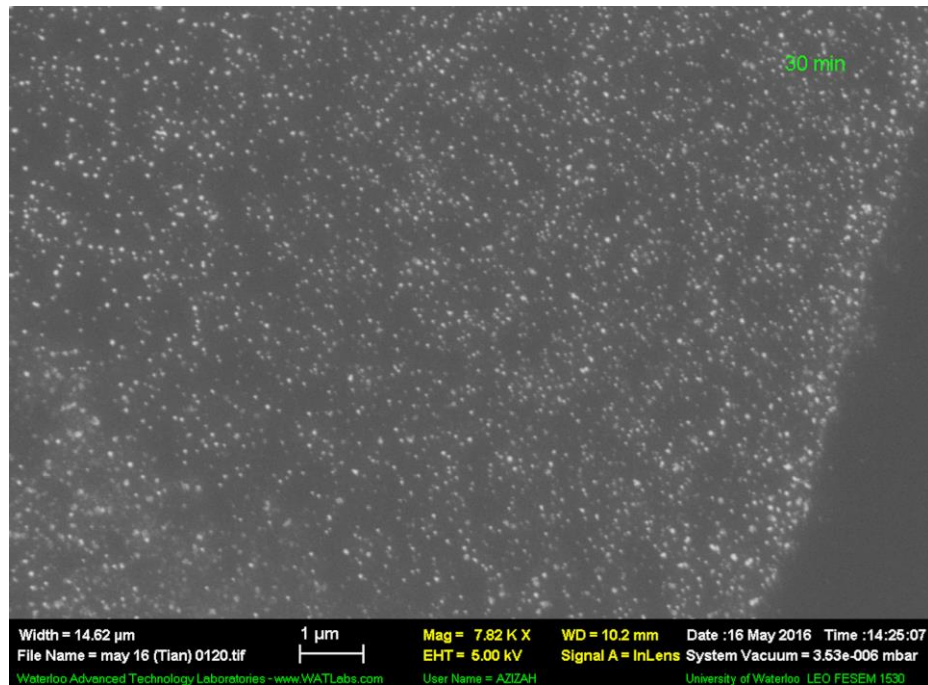


Figure 50: SEM image of etched is structure after RIE (treated time 30 minutes).

Chapter 3. Discussion and Findings

3.1 Coating PS-b-PMMA BCP Thin Film

As shown in figures 14 to 24, BCP thin films of PS-b-PMMA created perfect perpendicular lamellae structure in some cases, while other cases have shown some defects. These defects are probably due to one of following reasons: the film was too thick, the film was not-uniform, or the annealing time was too short. As discussed in chapter 1, the film thickness may also change the orientation of the BCP. Therefore, obtaining perpendicular BCP morphologies surface treatment is a must.

3.2 Coating PS-b-PMMA BCP Thin Film With A Surface Neutralizing Underlayer

One of the common methods to create natural surface for the perpendicular self-assembly of PS-b-PMMA block copolymer is the grafting of a random PMMA-r-PS copolymer brush with the same PS/PMMA ratio as the BCP. However, those random block copolymers with –OH terminated group are expensive and take a long time to be grafted. Due to these limitations, other alternative methods have been studied. In pervious chapters, we have summarized some of the most promising methods to achieve perpendicular orientation for the lamellar structures and surface neutralization. In the present work, we used the evaporation of 3MPTS, which is very efficient since only a very small volume of 3MPTS is used. This process is very fast and is capable of coating many substrates at the same time. This method is also free of contaminants in

comparison to the liquid coating process.

MPTS was chemically attached to the Silicon surface. Si substrate has a native oxide layer that helps 3-MPTS bonds to it. One of the chlorine atoms that is bonded to Si in the 3-MPTS reacts with the hydroxyl group on the substrate surface in which the oxygen form the surface bonds to the Si in the 3-MPTS and releasing HCl as a byproduct. Accordingly, washing with acetone only removes the 3-MPTS that are not chemically bonded to the substrate.

Silicon surface has relatively high surface energy (i.e hydrophilic) due to the native oxide layer naturally formed on the surface. The contact angle of a bare Si surface is approximately 40° . This hydrophilic surface attracts the PMMA chain in the block-co-polymer to wet it first. This gives us a horizontal lamella structure (Figure 53). However, after 3-MPTS treatment, the surface energy decreases which is evident by an increase in the contact angle to $65.14^\circ \pm 2.09$. The decrease in surface energy eliminates any surface preference to any polymer side of the block-co-polymer, which leads to a vertical lamella structure that is transferred to the fingerprint pattern after the second oxygen plasma RIE treatment.



Figure 51: a) Horizontal self-assembled lamella on a non-neutralized silicon surface. b) Vertical self-assembled lamella on a neutralized silicon surface (the green area represents 3-MPTS monolayer).

Si surface neutralizing enforces a vertical directionality to the formation of the lamella. Otherwise, the polymer layers in the horizontal lamella structure are etched layer-by-layer leaving a flat surface behind (Figure 53).

3.3 Varying The Annealing Time To Form Self-assembly of Block Copolymer

Various annealing times were used under constant annealing temperature. The main purpose of this experiments was to ensure that the fingerprint would not rapidly etch away by wet etching to increase the throughput of this process. From pervious chapter, for the constant temperature of 190°C we learned that to obtain good results, the annealing time is 15 minutes or higher. This annealing time produces well defined perpendicular lamellar structures; both SEM and AFM images confirm this finding.

3.4 Varying Soaking And RIE Etching Time

Various soaking times were used in this study. The main purpose was to determine the exact time to etch away the Al from the wafers. Etching time of Al was between 5 seconds and 1 minute. The purpose of exposure to oxygen gas was to remove all block copolymers, and the purpose of exposure to CF₄ was to slightly etch the silicon. SEM images in figures 25 to 50 show these results.

3.5 Conclusion

This study has shown an easy and fast way to achieve a perpendicular self-assembled pattern of PS-b-PMMA. The proposed method depends on neutralizing the surface using 3-MPTS by vapor deposition for 40 minutes to 2 hour at room temperature. The transfer pattern process was not successfully achieved using the mentioned method, however, this study paved the path towards improvements in future works.

Bibliography

1. B.babak, Morphology Control and Ordering of PS- b-PMMA Block Copolymer by The Use of Neutral Monolayer and E-beam Lithography, 2013.
2. X. Gu, I. Gunkel, T. P. Russell, and T. P. Russell, “Pattern transfer using block copolymers”, Journal of Mathematical-physical and engineering science, 2013.
3. Leibler L., “Theory of microphase separation in block copolymers”, Macromolecules, 13, 1602–1617, 1980. (doi:10.1021/ma60078a047)
4. W. Alyalak, “Block Copolymer Self-assembly and Graphene Dry Etching”, 2015.
5. Segalman, R. A., “Patterning with block copolymer thin films”, Materials Science and Engineering: Reports, 48(6), 191-226, 2005.
6. C. Park, J. Yoon, and E. L. Thomas, “Enabling nanotechnology with self-assembled block copolymer patterns,” Polymer (Guildf), vol. 44, no. 22, pp. 6725–6760, 2003.
7. A. P. Marencic and R. a. Register, “Controlling Order in Block Copolymer Thin Films for Nanopatterning Applications,” Annu. Rev. Chem. Biomol. Eng., vol. 1, no. 1, pp. 277–297, 2010.
8. 3 MPTS paper unpublished.
9. H. C. Kim, S. M. Park, W. D. Hinsberg, and I. R. Division, “Block copolymer based nanostructures: Materials, processes, and applications to electronics,” Chem. Rev., vol. 110, no. 1, pp. 146–177, 2010.
10. P. Mansky, T. Russell, C. Hawker, J. Mays, D. Cook, and S. Satija, “Interfacial Segregation in Disordered Block Copolymers: Effect of Tunable Surface Potentials,”

- Physical Review Letters, vol. 79, no. 2. pp. 237–240, 1997.
11. P. Mansky, T. P. Russell, C. J. Hawker, M. Pitsikalis, and J. Mays, “Ordered diblock copolymer films on random copolymer brushes,” *Macromolecules*, vol. 30, no. 22, pp. 6810–6813, 1997.
 12. R. D. Peters, X. M. Yang, T. K. Kim, B. H. Sohn, and P. F. Nealey, “Using self-assembled monolayers exposed to X-rays to control the wetting behavior of thin films of diblock copolymers,” *Langmuir*, vol. 16, no. 10, pp. 4625–4631, 2000.
 13. S. O. Kim, H. H. Solak, M. P. Stoykovich, N. J. Ferrier, J. J. De Pablo, and P. F. Nealey, “Epitaxial self-assembly of block copolymers on lithographically defined nanopatterned substrates,” *Nature*, vol. 424, no. 6947, pp. 411–414, 2003.
 14. E. Sivaniah, Y. Hayashi, S. Matsubara, S. Kiyono, T. Hashimoto, K. Fukunaga, E. J. Kramer, and T. Mates, “Symmetric diblock copolymer thin films on rough substrates. Kinetics and structure formation in pure block copolymer thin films,” *Macromolecules*, vol. 38, no. 5, pp. 1837–1849, 2005.
 15. T. Thurn-Albrecht, J. Derouchey, T. P. Russell, and H. M. Jaeger, “Overcoming interfacial interactions with electric fields,” *Macromolecules*, vol. 33, no. 9, pp. 3250–3253, 2000.
 16. T. Xu, Y. Zhu, S. P. Gido, and T. P. Russell, “Electric Field Alignment of Symmetric Diblock Copolymer Thin Films,” *Macromolecules*, vol. 37, no. 7, pp. 2625–2629, 2004.
 17. R. J. Albalak and E. L. Thomas, “Microphase separation of block copolymer solutions in a flow field,” *J. Polym. Sci. Part B Polym. Phys.*, vol. 31, no. 1, pp. 37–46, 1993
 18. M. Kimura, M. J. Misner, T. Xu, S. H. Kim, and T. P. Russell, “Long-range ordering of diblock copolymers induced by droplet pinning,” *Langmuir*, vol. 19, no. 23, pp. 9910–9913, 2003.

19. Y.-R. Hong, D. H. Adamson, P. M. Chaikin, and R. A. Register, "Shear-induced sphere-to-cylinder transition in diblock copolymer thin films," *Soft Matter*, vol. 5, no. 8, p. 1687, 2009.
20. B. C. Berry, A. W. Bosse, J. F. Douglas, R. L. Jones, and A. Karim, "Orientational order in block copolymer films zone annealed below the order-disorder transition temperature," *Nano Lett.*, vol. 7, no. 9, pp. 2789–2794, 2007.
21. Misra, A., Hogan, J. D., & Chorush, R., "Wet and Dry Etching Materials. Handbook of Chemicals and Gases for the Semiconductor Industry", (3), 1–5, 2002. Available: <https://doi.org/10.1002/0471263850.mis056>
22. L. Oria, A. Ruiz De Luzuriaga, J. A. Alduncin, and F. Perez-Murano, "Polystyrene as a brush layer for directed self-assembly of block co-polymers," *Microelectron. Eng.*, vol. 110, pp. 234–240, 2013.
23. L. C. by Geoffrey A Ozin, André Arsenault, "Nanochemistry: A Chemical Approach to Nanomaterials", 2008.
24. B. Sohn, "Perpendicular lamellae induced at the interface of neutral self-assembled monolayers in thin diblock copolymer films," *Polymer (Guildf)*, vol. 43, no. 8, pp. 2507–2512, 2002.